Soil Biology and Biochemistry 209 (2025) 109905

Contents lists available at ScienceDirect

Soil Biology and Biochemistry

journal homepage: www.elsevier.com/locate/soilbio

Impact of different soil erosion levels on gross N transformation processes and gaseous N losses: An incubation study

Julia Schoof [a,b,d,*], Maire Holz [a], Tobias Rütting [c], Reinhard Well [d], Caroline Buchen-Tschiskale [d]

[a] Leibniz Center for Agricultural Landscape Research (ZALF), Eberswalder Str. 84, Müncheberg, 15374 Germany
[b] Humboldt University of Berlin, Thaer-Institute of Agricultural and Horticultural Sciences, Unter den Linden 6, 10099 Berlin, Germany
[c] Department of Earth Sciences, University of Gothenburg, Box 460, 40530, Göteborg, Sweden
[d] Thünen Institute of Climate-Smart Agriculture, Bundesallee 65, 38116 Braunschweig, Germany

ARTICLE INFO

Keywords:
Gross N transformation rates
Topsoil erosion
Stable isotope techniques
^{15}N gas flux method
Nitrous oxide
Dinitrogen

ABSTRACT

Erosion is a key driver of topsoil removal in agriculture, resulting in nutrient losses and leaving truncated soil profiles on shoulder slopes, where subsoil material can be incorporated into topsoil by the plough, changing soil properties and, thus, altering biogeochemical cycling and associated nitrogen (N) losses. To date, the effects of topsoil erosion on N cycling have rarely been investigated. We conducted a short-term mesocosm experiment, integrating ^{15}N tracing techniques to quantify N transformation processes, focusing on N availability and N losses in three artificially eroded agricultural topsoils. Nitrogen transformation pathways were simulated using the numerical model *Ntrace*, considering N uptake by maize (*Zea mays* L.) at early development stages. The ^{15}N label also allows the quantification of nitrous oxide (N_2O) and dinitrogen (N_2) losses by applying the ^{15}N gas flux method (^{15}NGF).

Erosion induced topsoil dilution significantly reduced gross N turnover and consequently N_2O and N_2 emissions in both treatments with and without plants. The oxidation of ammonium (NH_4^+) to nitrate (NO_3^-) was by far the dominating N pathway across all investigated topsoils, followed by N_{org} mineralization > NH_4^+ immobilization. However, more than 90 % of total N_2O losses derived from the NO_3^- pool, with coupled nitrification-denitrification assumed to be the dominant process at water contents of ~40 % water-filled pore space (WFPS). Although maize more than doubled $N_2O + N_2$ emissions in some treatments, the overall effect of topsoil dilution on gaseous N losses was considerably greater, independent of maize presence. Our study contributes to a more comprehensive understanding of N cycling in erosion-affected agricultural soils, which is essential for enhancing N fertilizer use efficiencies and reducing N pollution.

1. Introduction

Erosion is a major process of soil redistribution that simultaneously leads to nutrient losses from agricultural fields and causes eutrophication in natural habitats, where the displaced nutrients accumulate (Berhe and Torn, 2017). The impact of soil erosion on soil properties is well described, whereby most studies in the last years focused on the effects of erosion on soil organic carbon (SOC) transformations and stocks (Van Oost et al., 2005, 2007; Berhe et al., 2012; Doetterl et al., 2016; Hoffmann et al., 2018) or the effect of erosion on greenhouse gas emissions (Reicosky et al., 2005; Wang et al., 2017; Gao et al., 2020; Vaidya et al., 2024). Fewer authors examined how erosion affects the terrestrial N cycle (Berhe et al., 2018; Quinton et al., 2010; Weintraub et al., 2015), although carbon (C) and nitrogen (N) cycles are strongly coupled (Holz and Augustin, 2021).

About half of the arable soils in Europe are prone to erosion (Borrelli et al., 2022). Initially recognized as a contributor to other erosion processes (Allmaras et al., 1967; Govers et al., 1994), tillage is now considered the second largest cause of soil erosion following the erosion by water in European agriculture (Borrelli et al., 2022; Ghotbi et al., 2023). During soil tillage, the transportation of soil material downslope leads to truncated topsoils at hill shoulders and can promote regular

* Corresponding author. Leibniz Center for Agricultural Landscape Research (ZALF), Eberswalder Str. 84, Müncheberg, 15374 Germany.
E-mail addresses: julia.schoof@zalf.de (J. Schoof), maire.holz@zalf.de (M. Holz), tobias.rutting@gvc.gu.se (T. Rütting), reinhard.well@thuenen.de (R. Well), caroline.buchen-tschiskale@thuenen.de (C. Buchen-Tschiskale).

https://doi.org/10.1016/j.soilbio.2025.109905
Received 13 March 2025; Received in revised form 1 July 2025; Accepted 4 July 2025
Available online 5 July 2025

incorporation of subsoil low in organic matter into the topsoil by the plough (Heckrath et al., 2005; Berhe et al., 2018). This process is referred to as topsoil dilution (Vaidya et al., 2024; Zentgraf et al., 2024), because the decline in soil organic matter (SOM), caused by the incorporation of subsoil in the topsoil is accompanied by a decrease in C and N contents and, hence, affects biogeochemical cycles (Berhe et al., 2018; Holz and Augustin, 2021).

Nitrogen is an essential macronutrient that is still a limiting factor for plant production in agriculture, even though it contributes to the pollution of natural ecosystems (Galloway et al., 2008). More than 90 % of the N in soil is part of SOM and becomes available to plants mainly by microbial-induced mineralization to soluble organic N forms and ammonium (NH_4^+) (Robertson and Groffman, 2015; Govindasamy et al., 2023). Recently, a diverse range of bacteria, archaea and fungi have been identified as capable of oxidizing these N compounds into different oxygen-containing N molecules, such as nitrous oxide (N_2O), nitric oxide (NO), nitrite (NO_2^-) and nitrate (NO_3^-), thereby increasing its oxidation state. These transformation processes occur through various energy-yielding autotrophic and heterotrophic pathways, many of which are still not completely understood, particularly with regard to the microbial groups and enzymes involved (Kuypers et al., 2018; Myrold, 2021). Key processes include aerobic NH_4^+ oxidation to NO_2^-, followed by its oxidation to NO_3^-. Reactions that are typically carried out by distinct groups of bacteria and archaea, and, further known to be an important source of NO and N_2O under aerobic conditions (Butterbach-Bahl et al., 2013; Medinets et al., 2015). More recently, it was observed that these transformation processes can also occur within a single microorganism, belonging to the group of complete ammonia oxidizers (*comammox*) (Daims et al., 2016; Li et al., 2019; Myrold, 2021).

Under oxygen (O_2)-limited conditions, O_2-containing inorganic N compounds can be used as electron acceptors via a series of reductive enzymatic steps and intermediates. In these steps NO, N_2O and dinitrogen (N_2) can be produced as by- or end products, which can be released from soil. Most of the microorganisms involved in these dissimilatory processes are facultative anaerobe and require C as an energy source (Firestone and Davidson, 1989; Khalil et al., 2004; Kuypers et al., 2018). Heterotrophic denitrification is considered the main source of N_2O and N_2 in fertilized soils under anaerobic conditions. This process can even occur in soils that appear well aerated, when O_2 is locally depleted by processes such as respiration or NH_4^+ oxidation, creating anaerobic zones particularly around organic particles or plant roots (Wrage et al., 2001; Azam et al., 2002; Butterbach-Bahl et al., 2013; Yang et al., 2021; Schlüter et al., 2024). Anaerobic microsites also sustain denitrification e.g. through the supply of C compounds from root exudates. Beside O_2 depletion, heterotrophic denitrification is determined by (1) the availability of oxygen-containing inorganic N compounds (NO_2^- and NO_3^-), which are used as alternative electron acceptors, (2) the availability and quality of C substrates, which are used as electron donors, and (3) the microbial community that conducts denitrification reactions (Schlüter et al., 2018; Myrold, 2021). Other processes that reduce NO_2^- and NO_3^- also contribute to the formation of N_2O and N_2 under similar environmental conditions. These include the dissimilatory nitrate reduction to ammonium (DNRA) (Tiedje, 1988; Rütting et al., 2011a; Schmidt et al., 2011; Chen et al., 2015; Putz et al., 2018), co-denitrification (Laughlin and Stevens, 2002; Spott et al., 2011; Spott and Stange, 2011; Medinets et al., 2015), anaerobic ammonium oxidation (*anammox*) (Spott and Stange, 2007; Long et al., 2013; Harris et al., 2015) and nitrifier denitrification (Kool et al., 2010; Zhu et al., 2013; Wrage-Mönnig et al., 2018). Chemodenitrification also contributes to the formation of NO and N_2O, when intermediates of NH_4^+ oxidation, such as NO_2^- accumulate in soils (Bremner, 1997; Heil et al., 2015). Apart from organic matter and high soil water content, this non-enzymatic process requires NH_4^+, amines or reduced metals (Medinets et al., 2015).

Microbial growth and activity in soil are limited by substrate availability (Booth et al., 2005; Soong et al., 2020). Consequently, erosion-induced topsoil dilution is likely to limit microbially driven N transformation processes, due to the limited availability of both C and N stored predominantly in SOM rich topsoil. This is in accordance with several studies, recording lower carbon dioxide (CO_2) and N_2O emissions in eroded soils compared to non-eroded soils (Gao et al., 2020; Vaidya et al., 2024). Due to limited soil N contents and low mineralization rates of SOM in eroded topsoils, the efficiency with which plants take up mineral N applied with synthetic fertilizer is expected to increase, as the uptake of soil-derived N is more restricted than in non-eroded topsoils (Pradhan et al., 1997; Malhi et al., 2004). However, plants affect N transformation processes by releasing root exudates into the rhizosphere (Herman et al., 2006; Holz et al., 2023). Therefore, it is likely that the presence of plants can partly counterbalance the low availability of substrate in eroded topsoils and therefore enhance N cycling. Furthermore, the incorporation of subsoil into topsoil can alter soil texture, therefore affecting the storage capacity for organic and inorganic N. For example, incorporation of clay-rich material can enhance its storage capacity for organic compounds and mineral N forms, such as NH_4^+, further protecting N from microbial and plant uptake (Castellano et al., 2012; Berhe et al., 2018; Zentgraf et al., 2024). Soil texture is also known to alter the diffusion properties of soils, thus determining O_2 penetration and N_2O diffusion from soils, and consequently its residence time, which directly affects the likelihood of further N_2O consumption (Butterbach-Bahl et al., 2013). There is evidence that microbial abundance and community composition can change throughout the soil profile, regulated by soil properties such as C and N availability, soil pH or water availability (Jones et al., 2018; Preusser et al., 2019), with microbial activity typically reduced in subsoil compared to topsoil (Doran, 1987; Li et al., 2014).

Although tillage erosion alters soil properties within agricultural fields, affecting N turnover and associated N losses, the impact of erosion-induced topsoil dilution on different N transformation processes is rarely investigated. Disentangling and quantifying the main processes, that determine the availability and loss of N compounds in agricultural soils, is still challenging due to the complexity of interactions and the metabolic versatility of microbes involved. Existing studies often only focus on individual aspects of the N cycle (Malhi et al., 2004; Han et al., 2017; Vaidya et al., 2023; Zentgraf et al., 2024), missing its interconnectedness and complexity. The present study aims to provide a more comprehensive overview of main N transformation processes in eroded soils, combining different stable isotope techniques in a mesocosm study design. Gross N transformation rates in artificially eroded topsoils are quantified using the numerical model *Ntrace* (Müller et al., 2004, 2007; Rütting and Müller, 2007) by ^{15}N-labelling either the NH_4^+ or the NO_3^- pool. The effects of plants and their N uptake on these N pools are also considered. Additionally, the ^{15}N label allows the quantification and partitioning of N_2O and N_2 generated from different processes, removing N either from the NH_4^+ or the NO_3^- pool, by application of the ^{15}N gas flux (^{15}NGF) method.

We hypothesize that (1) microbial-induced N transformation processes, such as gross N mineralization or gross NH_4^+ oxidation, decrease with increasing topsoil dilution along with the availability of substrates (C and N compounds). (2) Despite lower microbial activity and, therefore, lower biotic immobilization, gross N immobilization rates in eroded topsoils are comparable to those in non-eroded topsoils. This is because incorporation of clay with the subsoil material into the topsoil increases the abiotic N retention capacity of eroded topsoils. (3) Losses of N_2O, derived from the oxidation of NH_4^+, dominate gaseous N pathways under predominantly aerobic soil conditions. However, these losses steadily decrease with increasing erosion level due to lower NH_4^+ availability after topsoil dilution. In comparison, losses of N_2O and N_2 derived from the labelled NO_3^- pool (denitrification, nitrifier denitrification, coupled nitrification denitrification, co-denitrification) play a minor role in the production of gaseous N and are mainly limited by C availability and the occurrence of anaerobic microsites formed through

O_2-consuming processes. These requirements are more likely to be met in non-eroded topsoils than in eroded topsoils. (4) Plants affect N transformation processes by providing energy in the form of root exudates. Therefore, the presence of plants will partly counterbalance the low availability of substrate in eroded topsoils, reducing the effect of erosion on gross N transformation rates. However, soil-borne N remains significantly lower in eroded than in non-eroded topsoils, resulting in a higher plant N uptake from applied fertilizer.

2. Material and methods

We conducted a short-term mesocosm incubation experiment to assess the effect of erosion induced topsoil dilution and plant presence on N transformations and N fluxes under controlled conditions. We investigated three different erosion levels, which means different levels of subsoil admixture to the topsoil.

2.1. Soil properties and preparation

We collected topsoil (0–30 cm) and subsoil material (100–120 cm) from a *Nudiargic Luvisol* (IUSS Working Group, 2015) of the CarboZALF-D site (53°22′47″ N, 13°47′06″ E, MAT: 9.2 °C; MAP: 508 mm, 2005–2022) (Vaidya et al., 2024). This area, located within the ground moraine landscape of Brandenburg (Germany), is characterized by a hilly topography and intensive agriculture. The soil has been conventionally cultivated in the last years and primarily received mineral fertilizers, with spring barley grown before soil material was collected for the experiment.

Compared to the topsoil, the subsoil material was depleted in soil organic C (C_{org}) and total N (N_t) (Table 1), also shown in a reddish-brown color. The clay content of the subsoil is higher compared to the topsoil due to the transport of clay particles during soil development.

After soil sampling, soil was sieved field-fresh at 4 mm for homogenization. To enable microbes to adapt on changing environmental conditions, soil was adjusted to 30 % WFPS, 10 days prior to the experimental start. The soil was pre-incubated in the dark at a mean temperature of 18 °C. Water contents were checked every second day by weighing, and adjusted, if necessary, until the start of the experiment.

2.2. Experimental set up and ^{15}N-labelling of the soil

We simulated erosion induced topsoil dilution by mixing the topsoil material with varying amounts of subsoil material to create three artificial erosion levels, based on the approach of Zentgraf et al. (2024). The non-erosion level (E0) contained 100 % topsoil material and served as a control. The weakly (E1) and strongly (E2) erosion levels contained 80 % and 60 % topsoil, and the remaining amounts of subsoil.

We used a dual ^{15}N labelling approach, also referred to as mirror image approach (Watkins and Barraclough, 1996), for quantifying gross N transformation rates in the different treatments (Davidson et al., 1991; Müller et al., 2007; Rütting et al., 2011b). We labelled either the NH_4^+ pool or the NO_3^- pool of equal amounts of soil from each treatment using the stable isotope ^{15}N. The labelling was achieved by applying ammonium nitrate (NH_4NO_3) at a rate of 60 mg N kg^{-1} soil (98 atom %), containing either ^{15}N-enriched NH_4^+ or NO_3^-. The liquid fertilizer was evenly distributed by systematically mixing it several times with the different soil materials (topsoil and subsoil).

In order to enrich the soil material to a ^{15}N abundance of 50 atom %, the amount of required ^{15}N for each treatment was based on the initial NH_4^+-N and NO_3^--N contents of the soil material. For this, we took subsamples from the pre-incubated topsoil and subsoil four days before the experiment started. We then calculated the quantities of labelled and non-labelled fertilizer required to achieve the intended N enrichment in the mixture. This calculation was performed using the isotope dilution equation as outlined in IAEA (1983).

The incubation experiment was conducted in acrylic glass columns of 18 cm height and 14.3 cm diameter with four replicates. Each column was filled with 1.64 kg moist soil, representing the three different erosion levels (E0, E1, E2). Soil water content was increased to 40 % WFPS and soil was packed to a bulk density of 1.2 g cm^{-3}. Three maize seedlings each (*Zea mays* L., KWS OTTO), germinated for three days in the dark on moist paper at 27 °C, were planted in every second column (treatments E0p, E1p, E2p). Soil columns were then installed in a mesocosm facility, where they were connected to a gas mixing unit, enabling the continuous influx of N depleted air (20 % O_2, 0.5 % N_2, 350 ppm CO_2 and 250 ppb N_2O in He) at a flow rate of 10 ml min^{-1}, as described in detail in Kemmann et al. (2021). Conducting the experiment in this artificial atmosphere made the measurements of N_2 losses more precise. We illuminated the columns 12 h per day for optimal plant growth conditions and kept air temperature constant at 18 °C.

2.3. Gas sampling and analysis

At the start of the experiment, a total of 64 columns per treatment were installed in the mesocosm facility, representing four treatments (three erosion levels × plant presence/absence) with 16 replicates per treatment. CO_2 and N_2O losses were automatically measured in each column using a gas chromatograph (GC), equipped with an electron capture detector (ECD) and a thermal conductivity detector (TCD) (GC-2014, Shimadzu, Germany). Measurement intervals decreased with incubation time from every 7 h at the beginning of the experiment to every 2 h after seven days, as destructive soil sampling was conducted at distinct time points throughout the incubation period *(*see also *"Sample preparation")*. This reduced the number of replicates available for gas measurements over time. In total, four replicates remained after the penultimate sampling at 120 h of incubation. An empty column was installed for measurements of background concentration in the artificial atmosphere. Additionally, five calibration standards were measured regularly to assess the precision of the CO_2 and N_2O measurements.

Daily gas samples were collected from each treatment in 12 mL Exetainers for analysis of the N_2O and N_2 isotopic composition using a MAT 253 isotope ratio mass spectrometer (IRMS), equipped with a modified GasBench II preparation system and a PAL autosampler (Thermo Fisher Scientific, Germany). This system enables the direct measurement of the stable isotope ratios ^{29}R ($^{29}N_2/^{28}N_2$) and ^{30}R ($^{30}N_2/^{29}N_2$) of N_2, N_2+N_2O and N_2O, as previously described in detail by Lewicka-Szczebak et al. (2013). As the measurement method became inaccurate at low N_2O concentrations, some samples were additionally measured using a Delta V plus IRMS (Thermo Fisher Scientific, Germany), which was coupled to an automatic preparation system with Precon plus Trace GC Isolink (Thermo Scientific, Bremen, Germany), where N_2O was pre-concentrated, separated, and purified and m/z 44, 45, and 46 of the intact N_2O^+ ions were determined (Lewicka-Szczebak et al., 2014). ^{29}R and ^{30}R were derived from m/z 44, 45, and 46 (Bergsma et al., 2001). Typical repeatability for ^{29}R and ^{30}R was 6 × 10^{-6} and 2 × 10^{-6}. Data was normalized against background values of a breathing air laboratory standard.

Table 1
Soil characteristics separately for the topsoil and subsoil of the Nudiargic Luvisol used for the experiment (n = 3 for soil pH; n = 1 for all other soil properties).

	depth [cm]	sand [%]	silt [%]	clay [%]	C_{org} [%]	N_t [%]	C:N ratio	pH_{CaCl2}
Topsoil	0–30	61.27	25.45	13.28	0.87	0.09	9.77	6.42
Subsoil	100–120	52.62	29.67	17.71	0.18	0.03	6.20	6.70

2.4. Soil and plant sampling and analysis

2.4.1. Sample preparation

We took soil and plant samples after 1 h, 24 h, 48 h, 72 h and 168 h of incubation for observing changes in the different mineral N pools over time. The higher sampling frequency at the beginning of the experiment was chosen in order to record rapid changes in gross N mineralization rates immediately after fertilization (Kirkham and Bartholomew, 1954). Incubation stopped after 168 h, to avoid underestimation of N transformation due to remineralization of the labelled N that again enters the NH_4^+ pool (Murphy et al., 2003). Plants, harvested after 72 h and 148 h, were already large enough to allow separate analysis of aboveground (shoots) and belowground biomass (roots).

Soil and plant material was dried at 60 °C for 48 h for the analysis of C_{org} and N_t contents. For the analysis of the NH_4^+-N and NO_3^--N contents in the fresh soil samples, as well as its ^{15}N abundances, we extracted 300 g moist soil with 600 ml of a 2 M potassium chloride (KCl) solution (1:2 ratio) by shaking the suspension for 1 h, following the extraction procedure in ISO (2005). Simultaneously, 50 g soil was weighed for estimation of gravimetric water contents by drying at 105 °C until constant weight. Soil extraction was performed immediately after soil sampling, to avoid further microbial activity, and four aliquots of the extracts were frozen at −18 °C until analysis took place.

2.4.2. Sample analysis

Contents of NH_4^+-N and NO_3^--N in the extracts were estimated photometrically using a Continuous-Flow-Analyzer (CFA San++ Skalar, Netherlands). The ^{15}N abundances were measured using a SPIN-MIRMS device. The SPIN unit is an automated sample preparator, which enables the conversion of NO_3^- and NH_4^+ in the liquid sample to N_2O and N_2, respectively. The unit is connected to a membrane inlet isotope ratio mass spectrometry (Delta plus, Thermo Fisher Scientific, Germany) via a ConFlo III interface that allows the determination of the ^{15}N abundance in the sample (Dyckmans et al., 2021). The analytical precision was determined by repeated measurements of standards and was consistently <0.02 atom %, <0.01 atom % and <1.5 atom % ^{15}N for the 5 atom %, 10 atom % and 50 atom % standard, respectively.

For the estimation of C_{org} and N_t contents, as well as its ^{15}N abundances, in the ground soil and plant material we used an elemental Analyzer Flash 2000, coupled to a Delta V isotope ratio mass spectrometer (Thermo Fisher Scientific, Germany). Calibration standards were regularly measured to obtain precise analysis results. The precision was <0.2 % for C_{org}, <0.02 % for N_t and <0.08 atom % for ^{15}N.

2.5. Calculations and statistics

2.5.1. Calculating fluxes of N_2O, N_2 and CO_2

We started measuring gases in the mesocosm facility, as soon as, we set up the sealed columns for the experiment. However, we excluded data recorded 3 h after the installation, as we wanted to ensure that each column was filled properly with the N_2-depleted air. Each column was flushed with the artificial air from the gas mixing unit to accelerate the complete gas exchange. In general, it is recommended to exclude data from the initial 24-h period, due to an increase in mineralization resulting from mixing, aeration, and subsequent stimulation of microbial activity (Rohe et al., 2021). However, we retained and analyzed this data, as we wanted to examine the effects of tillage induced topsoil dilution under soil moisture and temperature conditions typically found at the beginning of the growing season. Observations with N_2 concentrations exceeding 5 % and flow rates exceeding 12 ml min^{-1} were excluded from further analysis, as this was an indication for column leakages.

Gas fluxes were derived from the measured concentrations of CO_2 and N_2O using the ideal gas law, considering an incubation temperature of 18 °C and an air pressure of 1 bar, as outlined in Kemmann et al. (2023). In the first step, the mass concentration C (mg CO_2–C L^{-1} or mg N_2O–N L^{-1}) was calculated by:

$$C = n \cdot \frac{M \cdot 273.15\ K}{22.4136\ \frac{L}{mol} \cdot (273.15\ K + T)} \tag{1}$$

where M is the molar mass of CO_2 or N_2O in g mol^{-1}, and T the incubation temperature during the experiment in °C. In a second step, CO_2 and N_2O fluxes were calculated by multiplying the mass concentration with the flow rate, and then dividing by the surface area of the soil within the column:

$$f = \frac{C \cdot 10^{-3} \cdot Q}{A} \tag{2}$$

where Q is the flow rate in mL h^{-1} and A is the soil surface area in m^2. For the estimation of cumulative fluxes, we used the trapezoidal rule to interpolate between the measurements and summed up the results.

We followed the approach of Spott et al. (2006) to determine the fractions of N_2 (fp_N_2), N_2+N_2O (fp_N_2+N_2O) and N_2O (fp_N_2O) originating from the ^{15}N-labelled pools. For a comprehensive understanding of the calculation methodology, we refer to other studies that provide detailed descriptions (Spott et al., 2006; Buchen et al., 2016; Well et al., 2019; Kemmann et al., 2021; Pfülb et al., 2024). In the following the index fp refers to N_2O and N_2 losses from the labelled pool (fp_N_2O and fp_N_2), as previously defined in other studies (Kemmann et al., 2021; Buchen-Tschiskale et al., 2023; Pfülb et al., 2024). For N_2O this includes losses from both the NO_3^- and the NH_4^+ pool, as both were labelled in separate treatments in this experiment. In order to distinguish N_2O losses from the NO_3^- pool from those from the NH_4^+ pool, we have introduced a new calculation procedure (see below) and extended the index to fp_N_2O_{NO3} and fp_N_2O_{NH4}, respectively. The index fp_N_2 has not been extended, as it always refers only to the N_2 losses from the labelled NO_3^- pool. The calculations are explained in the following sections, separately for both ^{15}N-labelled treatments: $NH_4^{15}NO_3$ and $^{15}NH_4NO_3$. Calculations in this study were based on combining fractions from IRMS analysis (fp) with total N_2O fluxes measured by the GC. This approach is preferable, when pool-derived N_2O and N_2 losses are close to the IRMS detection limit, which is generally higher than that for total N_2O losses measured by GC (Pfülb et al., 2024).

2.5.1.1. Calculating source-related N_2O and N_2 losses in $NH_4^{15}NO_3$ treatments.

In the $NH_4^{15}NO_3$ treatments, the measured ^{15}N abundances of the soil NO_3^- and NH_4^+ pools showed no remineralization of ^{15}N-labelled NO_3^- into the non-labelled NH_4^+ pool over time (Fig. S10). Therefore, we assumed that N_2O losses from the labelled pool, obtained by IRMS analysis, derived only from the NO_3^- pool in these treatments (fp_N_2O_{NO3}). Calculation of fp_N_2O_{NO3} was performed by combining the share of N_2O derived from the NO_3^- pool relative to total N_2O losses (Fp_N_2O_{NO3}), measured by IRMS, with total N_2O losses (N_2Ot) measured by the GC, as previously described by Pfülb et al. (2024) as follows:

$$fp\_N_2O_{NO3} = Fp\_N_2O_{NO3} \cdot N_2Ot \tag{3}$$

N_2O losses from other sources (fn_N_2O) were then calculated by subtracting fp_N_2O_{NO3} from total N_2O losses (N_2Ot) expressed as:

$$fn\_N_2O = N_2Ot - fp\_N_2O_{NO3} \tag{4}$$

To estimate the fraction of N_2O and N_2 losses derived from the NO_3^- pool (fp_N_2O + $N_{2,\ NO3}$), we divided the calculated fp_N_2O_{NO3} (Eq. (3)), based on combined GC and IRMS data, by the ratio of fp_N_2O to fp_N_2O + N_2 (N_2Oi). The latter were obtained directly from IRMS measurements of N_2O + N_2 isotopologues ^{29}R ($^{29}N_2/^{28}N_2$) and ^{30}R ($^{30}N_2/^{29}N_2$) (for more details on measurement and calculation procedure see e.g. Lewicka-Szczebak et al., 2013; Kemmann et al., 2021).

$$fp\_N_2O + N_{2,NO3} = \frac{fp\_N_2O_{NO3}}{N_2O_i} \tag{5}$$

where N_2Oi is the $N_2O/(N_2O + N_2)$ ratio of denitrification, which was calculated for each treatment and each sampling event (1 h, 24 h, 48 h, 96 h and 168 h of incubation) and additionally for the cumulative fluxes for all treatments as follows:

$$N_2Oi = \frac{fp\_N_2O_{IRMS}}{fp\_N_2O + N_{2,IRMS}} \tag{6}$$

where $fp\_N_2O + N_{2,\ IRMS}$ and $fp\_N_2O_{IRMS}$ are the losses of $N_2O + N_2$ and N_2O from the NO_3^- pool, obtained from IRMS analysis (calculation procedure described in detail e.g. by Kemmann et al. (2021)). Values of fp_N_2+N_2O that were below detection were set to half of the limit of detection (LOD). LOD was calculated by 4 x standard deviation (SD) for ^{29}R and ^{30}R. Losses of N_2 that derived from the NO_3^- pool, were calculated as formulated by:

$$fp\_N_2 = fp\_N_2O + N_{2,NO3} - fp\_N_2O_{NO3} \tag{7}$$

2.5.1.2. Calculating source-related N_2O and N_2 losses in $^{15}NH_4NO_3$ treatments. For the $^{15}NH_4NO_3$ treatments the IRMS analysis gives fp values (fp_N_2O and $fp\_N_2O + N_2$) describing the gaseous N losses from the NO_3^- and NH_4^+ pools as both pools might be ^{15}N-labelled due to ongoing nitrification. The NH_4^+ pool was actively labelled by the application of $^{15}NH_4NO_3$. However, the NO_3^- pool was ^{15}N-enriched over time by the production of new NO_3^- through oxidation of the labelled NH_4^+ (nitrification), which was indicated by an increase in $^{15}N–NO_3^-$ abundances (15a_NO_3) and subsequent decrease in $^{15}N–NH_4^+$ abundances (15a_NH_4) over time (Fig. S10). Both N pools can be a source of N_2O emissions, combined in fp_N_2O and $fp\_N_2O + N_2$, obtained from IRMS analysis in the $^{15}NH_4$-labelled treatments. To separate the two sources of labelled N_2O ($fp\_N_2O_{NO3}$ and $fp\_N_2O_{NH4}$), information on N_2O losses from the $^{15}NO_3$-labelled treatments and on the ^{15}N enrichment of the soil mineral N pools were combined.

Losses of N_2O, derived from the NO_3^- pool were calculated by multiplying N_2Ot by mean $Fp\_N_2O_{NO3}$ values of the $^{15}NO_3$-labelled treatment as follows:

$$fp\_N_2O_{NO3} = Fp\_N_2O_{NO3,mean} \cdot N_2Ot \tag{8}$$

where $Fp\_N_2O_{NO3,\ mean}$ is the mean of $Fp\_N_2O_{NO3}$ from the $^{15}NO_3$-labelled treatments, calculated separately for each sampling event and erosion level for the treatments with and without maize. To calculate the N_2O losses derived from the NH_4^+ pool ($fp\_N_2O_{NH4}$), the share of N_2O derived from the NH_4^+ pool relative to total N_2O losses ($Fp\_N_2O_{NH4}$), was first calculated as follows:

$$Fp\_N_2O_{NH4} = \frac{(15a\_N_2O - 0.003663) - ((15a\_NO_3 - 0.003663) * Fp\_N_2O_{NO3,mean})}{15a\_NH_4} \tag{9}$$

where 15a_N_2O is the ^{15}N abundance of N_2O, and 15a_NO_3 and 15a_NH_4 are the ^{15}N abundances of the soil NO_3^- and NH_4^+ pool, respectively, measured by SPIN-MIRMS. Values of $Fp\_N_2O_{NO3,\ mean}$ were again estimated from $Fp\_N_2O_{NO3}$ values of the $^{15}NO_3$-labelled treatments.

Negative values of $Fp\_N_2O_{NH4}$ occurred in cases where the 15a_NH_4, 15a_NO_3 and 15a_N_2O were <10 atom %, and the ^{15}N-abundances in the soil exceeded the ^{15}N-abundances of the measured N_2O. This can be explained by small inaccuracies of the different applied measurement techniques (IRMS, SPIN-MIRMS). Negative values were only observed after 168 h incubation, when N_2O losses as well as soil NH_4^+-N contents were at a low level. We used mean values of the same treatment to estimate $Fp\_N_2O_{NH4}$ if negative values were calculated. For some observations the sum of $Fp\_N_2O_{NO3,\ mean}$ and $Fp\_N_2O_{NH4}$ exceeded 1, indicating that the relative shares of both N_2O pools together were higher than 100 %. In those cases, $Fp\_N_2O_{NH4}$ were estimated by:

$$Fp\_N_2O_{NH4} = 1 - Fp\_N_2O_{NO3,mean} \tag{10}$$

Equation (10) is a simplification and was used under the assumption that no N_2O originated from sources other than the NO_3^- and NH_4^+ pools.

Values of $fp\_N_2O_{NH4}$ were then calculated by multiplying $Fp\_N_2O_{NH4}$ with N_2Ot, as for $fp\_N_2O_{NO3}$ in Equation (3):

$$fp\_N_2O_{NH4} = Fp\_N_2O_{NH4} \cdot N_2Ot \tag{11}$$

The losses of N_2O, which originate from sources other than the labelled NH_4^+ and NO_3^- pools, have been calculated as follows:

$$fn\_N_2O = N_2Ot - fp\_N_2O_{NO3} - fp\_N_2O_{NH4} \tag{12}$$

The calculation of fp_N_2 for the $^{15}NH_4$-labelled treatments was performed as follows:

$$fp\_N_2 = fp\_N_2O + N_{2,NO3+NH4} - fp\_N_2O_{NO3+NH4} \tag{13}$$

where $fp\_N_2O + N_{2,\ NO3+NH4}$ and $fp\_N_2O_{NO3+NH4}$ are the fp values, calculated based on Equation (5) and Equation (6), except that N_2O losses may originate from both the NO_3^- and NH_4^+ pools. As N_2Oi is calculated on the basis of N_2O and $N_2O + N_2$ from the NO_3^- pool only, it cannot be calculated directly from IRMS-values obtained for the $^{15}NH_4NO_3$ treatments. In these treatments losses of N_2O and combined $N_2O + N_2$ included those originating from the NH_4^+ pool. Estimating the denitrification ratio (N_2Oi), which accounts only for N_2O losses from the NO_3^- pool, would have introduced uncertainties and therefore was not carried out for the $^{15}NH_4NO_3$ treatments.

2.5.2. Calculating gross N transformation rates using the Ntrace model

We used information on NH_4^+-N and NO_3^--N contents, as well as their respective ^{15}N enrichments to calculate mean gross N transformation rates for each treatment using the *Ntrace* model (Müller et al., 2004, 2007; Rütting and Müller, 2007; Rütting et al., 2011b). The model integrates ^{15}N dilution and ^{15}N tracing concepts to quantify multiple N fluxes in the soil, including mineralization of organic N compounds to NH_4^+, immobilization of NH_4^+ and NO_3^- by microbial and plant uptake, oxidation of organic N compounds or NH_4^+ to NO_3^-, and the dissimilatory reduction of NO_3^- to NH_4^+. In total, the basic model consisted of four N pools and eight N transformation processes at the beginning of the model run. The *Ntrace* model further distinguishes between the slowly changing recalcitrant organic N pool (N_{rec}) and the active labile organic N pool (N_{lab}), in line with previously studies (Müller et al., 2011; Inselsbacher et al., 2013).

Initial conditions, comprising NH_4^+-N and NO_3^--N contents from the two ^{15}N-labelled treatments and their corresponding ^{15}N abundances across the five sampling events, were required to start the model run. The estimation of contents immediately after tracer application (t = 0 h) was done by linear back-extrapolation following Müller et al. (2004). The N transformation processes were described by zero or first order kinetics. To calculate average gross rates of N transformations following a first order kinetic, we interpolated model results across time and divided by the incubation time (Rütting and Müller, 2007).

The *Ntrace* model was addressed via MATLAB version 9.10.0.1710957 (R2021a) (The MathWorks Inc, 2021). In order to find the global minimum in the model space, we used an optimization algorithm based on a Markov Chain Monte Carlo sampling design. This

Bayesian technique is fast even at a high number of parameters and enables the determination of probability density functions (PDF) during the model run (Müller et al., 2007; Rütting and Müller, 2007). Thus, additional information regarding the accuracy of the parameters was provided by evaluating error covariances and the deviations from normal distribution. The optimal model was selected by minimizing the quadratic deviation of the modeled and the true value (*misfit* function), and the selection of parameters was done based on the Akaike Information Criterion (AIC) as described in detail by Rütting and Müller (2007).

2.5.3. Calculating ^{15}N recovery

In order to examine the effect of soil erosion level and plant presence on fertilizer N uptake, different isotope-based indices were calculated following IAEA (1983). For assessing the effect of different erosion levels on plant N uptake, the N derived from the fertilizer (Ndff) was calculated for the different erosion levels over the entire incubation as follows:

$$\mathrm{Ndff} = \frac{^{15}\mathrm{N\ atom\ \%\ excess\ in\ plant}}{^{15}\mathrm{N\ atom\ \%\ excess\ in\ fertilizer\ N}} \cdot 100 \tag{14}$$

The ^{15}N excess was calculated by subtracting the ^{15}N natural abundance of 0.3663 atom % from the measured ^{15}N abundance in the respective pool. As either NO_3^- or NH_4^+ was ^{15}N-labelled in the fertilizer, the Ndff refers to the respective pool and represents the N derived either from the NO_3^- or the NH_4^+ pool of the NH_4NO_3 fertilizer in this experiment. The Ndff is a relative proportion (%) that is independent from the absolute N content of the plant and, therefore, enables the comparison of the fertilizer-derived N-uptake for the different erosion levels.

Furthermore, we calculated ^{15}N recoveries of the fertilizer into the different N pools as follows (Barraclough, 1995; Buchen-Tschiskale et al., 2023):

$$^{15}\mathrm{N}_{\mathrm{recovery}} = \frac{^{15}\mathrm{N}_{\mathrm{recovered}}}{^{15}\mathrm{N}_{\mathrm{applied}}} \cdot 100 \tag{15}$$

where $^{15}N_{recovered}$ in % was calculated by summing the amount of ^{15}N in the different pools (NH_4^+-N, NO_3^--N, N_{org}, N_t in shoot and root of the maize) and the ^{15}N losses via N_2O and N_2. The $^{15}N_{applied}$ was estimated by multiplication of the ^{15}N enrichment of either NO_3^- or NH_4^+ of the fertilizer with the applied N.

2.5.4. Data analysis and statistics

The full data set was characterized by a 2-factorial design with 8 replicates, of which each 4 replicates were labelled either with $^{15}NH_4NO_3$ or $NH_4^{15}NO_3$ fertilizer. All calculations were performed using R version 4.3.1 (R Core Team, 2023). All graphics were created using the R package *ggplot* (Wickham, 2016). For the analysis of mean differences of general soil properties, cumulated gaseous losses (N_2O, N_2, CO_2) and the Ndff, we conducted a two-way analysis of variance (ANOVA) with the factors: erosion level and plant presence. The differences were examined based on Tukey-HSD tests with a significance level of $p < 0.05$ using the R package *emmeans* (Lenth, 2023) for balanced data sets. Residuals were inspected using the Kolmogorov-Smirnov test and the Levene test of the *car* package (Fox and Weisberg, 2019) for assessing normal distribution and variance homogeneity, respectively. If required, cumulative gas fluxes were log10 transformed to meet ANOVA assumptions. For evaluating treatment effects on gross N transformation rates, we calculated 85 % confidence intervals and compared them across treatments, as recommended by Rütting and Müller (2007). Overlapping confidence bands were considered to show non-significant differences between different groups. This procedure was recommended by Payton et al. (2000) for numerical model results based on a high number of iterations.

3. Results

3.1. Soil properties

Organic C contents decreased steadily with increasing erosion level with values of 8.46 ± 0.19 g C kg^{-1} for E0, 7.09 ± 0.52 g C kg^{-1} for E1 and 5.65 ± 0.24 g C kg^{-1} for E2 at the beginning of the incubation (Table S1). Same trend was observed for N_t, showing mean values of 0.95 ± 0.02 g N kg^{-1}, 0.82 ± 0.04 g N kg^{-1} and 0.65 ± 0.03 g N kg^{-1} for E0, E1 and E2, respectively. Contents of C_{org} and N_t differed significantly between the treatments and remained almost constant throughout the experiment. Water contents were adjusted to approximately 42 % WFPS, and decreased slightly during incubation to about 41 % WFPS (Table S1).

3.2. ^{15}N recovery

Total ^{15}N recovery was 89.41 ± 20.01 % (E0, E0p), 82.71 ± 8.80 % (E1, E1p) and 86.77 ± 5.96 % (E2, E2p) after 1h of incubation, when samples were taken for the first time after application of the ^{15}N-labelled fertilizer (*data not shown*). No differences between the different tracers ($^{15}NH_4NO_3$, $NH_4^{15}NO_3$) or the different soil erosion levels (E0, E1, E2, E0p, E1p, E2p) were observed over time (Table S2). Total ^{15}N-recovery remained almost constant throughout the 7-days incubation. However, the distribution of ^{15}N across different N pools changed over time, as plants continuously took up ^{15}N from the fertilizer, and gaseous N losses occurred throughout the experiment (Table S2). A tendency of increasing recovery rates with erosion level was observed for both

Table 2
Recovery of ^{15}N added either in the form of $^{15}NH_4NO_3$ ($^{15}NH_4^+$) or $NH_4^{15}NO_3$ ($^{15}NO_3^-$) across different N pools (maize aboveground and belowground biomass N, $N_2O + N_2$ emissions ($N_2O + N_2$) and total soil N (soil N_t)) after 7 days of incubation. Values represent treatment means ± standard deviation (n = 4). Different letters indicate significant differences between the studied erosion levels (E0 = non eroded, E1 = weakly eroded, E2 = strongly eroded) (lowercase letters) and treatments with (E0p, E1p, E2p) and without maize (E0, E1, E2) (capital letters) according to ANOVA followed by Tukey's HSD test ($p < 0.05$).

Treatment	Tracer	^{15}N recovery of the labelled NH_4NO_3 [%]				Total ^{15}N recovery [%]
		Aboveground biomass N	Belowground biomass N	$N_2O + N_2$	Soil N_t	
E0	$^{15}NO_3^-$	n.d.	n.d.	2.92 ± 0.74 a A	86.31 ± 3.59 a A	89.23 ± 3.67 a A
E1	$^{15}NO_3^-$	n.d.	n.d.	0.88 ± 0.58 b A	97.25 ± 10.03 a A	98.13 ± 9.48 a A
E2	$^{15}NO_3^-$	n.d.	n.d.	0.24 ± 0.10 c A	89.96 ± 7.71 a A	90.2 ± 7.73 a A
E0p	$^{15}NO_3^-$	1.89 ± 0.49 a	0.65 ± 0.18 a	6.02 ± 2.07 a B	72.72 ± 6.72 a B	81.27 ± 5.22 a A
E1p	$^{15}NO_3^-$	2.22 ± 0.34 a	1.34 ± 0.48 a	1.32 ± 0.42 b B	84.00 ± 5.90 a B	88.88 ± 5.46 a A
E2p	$^{15}NO_3^-$	4.10 ± 1.65 b	1.82 ± 0.89 b	0.55 ± 0.22 c B	95.24 ± 6.37 a B	101.70 ± 8.68 a A
E0	$^{15}NH_4^+$	n.d.	n.d.	1.80 ± 0.78 a A	89.63 ± 4.14 a A	91.43 ± 4.14 a A
E1	$^{15}NH_4^+$	n.d.	n.d.	0.56 ± 0.21 b A	82.80 ± 8.23 a A	83.36 ± 8.44 a A
E2	$^{15}NH_4^+$	n.d.	n.d.	0.11 ± 0.08 c A	93.68 ± 9.17 a A	93.79 ± 9.16 a A
E0p	$^{15}NH_4^+$	2.16 ± 0.63 a	0.86 ± 0.24 a	3.24 ± 0.31 a B	88.45 ± 8.35 a B	94.70 ± 8.08 a A
E1p	$^{15}NH_4^+$	1.56 ± 0.27 a	0.70 ± 0.14 a	1.64 ± 0.81 b B	72.68 ± 4.30 a B	76.58 ± 4.43 a A
E2p	$^{15}NH_4^+$	3.98 ± 1.58 b	1.87 ± 0.89 b	0.93 ± 0.40 c B	73.89 ± 3.54 a B	80.68 ± 3.07 a A

n.d. = not determined.

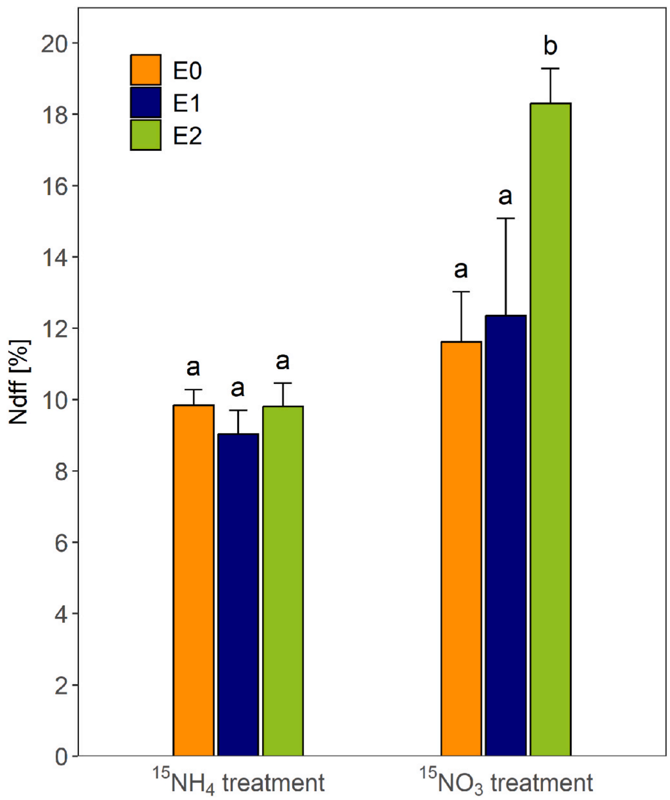

Figure 1. Shares of N derived from fertilizer (Ndff) in the maize biomass (below- and aboveground material). Fertilizer was applied as either $^{15}NH_4NO_3$ (left) or $NH_4^{15}NO_3$ (right) to topsoils of different erosion levels (E0p = non eroded, E1p = weakly eroded, E2p = strongly eroded). Different letters denote significant differences between treatments according to ANOVA followed by Tukey's HSD test ($p < 0.05$, $n = 4$).

above- and belowground biomass (Table 2). However, significant differences from the non-eroded control were only found for the strongly eroded treatment (E2p). Recovery of ^{15}N in $N_2O + N_2$ varied among the three soil treatments and was significantly influenced by both the degree of erosion and the presence of maize plants.

Maize plants continuously took up N from the applied fertilizer after 48 h of incubation, with around 10 % of this N coming from the labelled NH_4^+ pool by the end of the experiment (Fig. 1, Fig. S1). Values of $Ndff_{NH4}$ ranged from 8.17 % to 10.37 %, showing no significant differences between the different soil treatments (E0p, E1p, E2p). In contrast, the $Ndff_{NO3}$ increased with increasing erosion level (E0p < E1p < E2p), with no significant differences between the non-eroded (E0p) and slightly eroded (E1p) soils (Fig. 1).

3.3. Mineral N, gross N transformation rates and plant N uptake

The highest amount of NO_3^--N and NH_4^+-N was found in the non-eroded soils and generally decreased with increasing erosion level following the order E0 > E1 > E2, irrespective of whether maize was planted or not (Table S3). The NO_3^--N contents averaged 4.15 ± 0.17 µmol N g^{-1} in non-eroded topsoils (E0, E0p), 3.66 ± 0.10 µmol N g^{-1} in weakly eroded topsoils (E1, E1p) and 3.22 ± 0.11 µmol N g^{-1} in strongly eroded topsoils (E2, E2p) in samples taken 1h after mixing it with the labelled fertilizer. Differences in NH_4^+-N contents were more pronounced than differences in NO_3^--N contents (Table S3). The same trend in the NO_3^--N and NH_4^+-N contents was observed at the end of the incubation, where NO_3^--N contents generally increased, while NH_4^+-N contents decreased exponentially, approaching the detection limit.

Because we aimed to label the manipulated topsoils of different erosion levels to a ^{15}N abundance of 50 atom %, differences in initial ^{15}N

Table 3
Gross N transformation rates over the 7-days incubation period of soils of different erosion levels (E0 = non eroded, E1 = weakly eroded, E2 = strongly eroded), planted with (E0p, E1p, E2p) or without maize (E0, E1, E2), calculated by integrating rates provided by the Ntrace model over time, divided by the total time. Values represent treatment means ± standard deviation (n = 4). n.d. refers to not determined, including processes with gross rates that were indistinguishable from zero and therefore excluded from the final model run. Different letters indicate significant differences between the treatments, which are defined as non-overlapping 85 % confidence intervals.

N transformation process		Kinetics[+]	N transformation rate [µg N kg^{-1} d^{-1}]					
			E0	E1	E2	E0p	E1p	E2p
M_{Norg}	Mineralization of organic N to NH_4^+-N[a]	0/1	739.2 ± 79.6 a	470.4 ± 35.3 c	504.0 ± 24.45 c	672.0 ± 58.7 ab	134.4 ± 10.7 d	638.4 ± 21.5 b
I_{NH4_Nlab}	Immobilization of NH_4^+-N into labile organic N	1	268.8 ± 83.2 a	n.d.	n.d.	571.2 ± 66.7 b	n.d.	n.d.
O_{NH4}	Oxidation of NH_4^+ to NO_3^-	1	3897.6 ± 72.8 a	2654.4 ± 32.78 c	2116.8 ± 36.49 f	3528.0 ± 69.9 b	2486.4 ± 33.6 d	2251.2 ± 35.28 e

[+] 0 = zero-order kinetics, 1 = first-order kinetics.
[a] including mineralization of labile (M_{Nlab}) and recalcitrant (M_{Nrec}) organic N, described by first and zero order kinetic, respectively.

abundances between treatments were marginal. The labelled pools showed an increasing dilution of ^{15}N abundances over the incubation time, regardless of whether $NH_4^{15}NO_3$ or $^{15}NH_4NO_3$ was applied to the soil (Fig. S10). The $^{15}NH_4$-labelled treatment showed an exponential increase in ^{15}N abundances within the NO_3^- pool, indicating that $^{15}NH_4^+$ was oxidized to $^{15}NO_3^-$. In comparison, no ^{15}N entered the non-labelled NH_4^+ pool in the $^{15}NO_3^-$ treatments, as the ^{15}N abundances remained at natural abundance levels. This has been confirmed for treatments with and without maize.

The final *Ntrace* models fitted well with the measured NO_3^--N and NH_4^+-N concentrations and the corresponding ^{15}N abundances across all the investigated treatments (Figure S4 to Figure S9). The fitted models included three N transformation processes for the non-eroded treatment and two for the two eroded treatments, irrespective whether maize was planted or not (Table 3). For the comparison of gross N transformation rates, we combined the recalcitrant (M_{Nrec}) and the labile organic N (M_{Nlab}) into a single organic N pool, as M_{Nrec} was only significant in the E1p treatment. In general, gross NH_4^+ oxidation to NO_3^- (O_{NH4}) clearly dominated N transformation in all treatments, showing decreasing rates with increasing erosion level in the order E0 > E0p > E1 > E1p > E2p > E2. Differences between the erosion levels were significant, as shown by non-overlapping 85 % confidence intervals (Table 3). In total, gross NH_4^+ oxidation was reduced by maxima of 45.7 % in E2 and 36.2 % in E2p compared to the non-eroded controls E0 and E0p, respectively. Gross mineralization rates to NH_4^+ (M_{Norg}) also decreased with increasing erosion level, generally following the order E0 > E0p > E2p > E2 > E1 > E1p. In comparison to O_{NH4} and $M_{Norg,}$ immobilization of NH_4^+ (I_{NH4}) was only observed in the non-eroded treatments irrespective of maize presence, whereas in eroded topsoils I_{NH4} was too low to be detected by the *Ntrace* model. Differences between E0 and E0p were significant and showed highest rates in the treatments with maize (Table 3). All other N fluxes that can be quantified by *Ntrace* were excluded from the final model, as they did not show a detectable effect on N cycling in this experiment. This was also true for the NO_3^--N and NH_4^+-N uptake by plants, likely because N uptake by the young maize plants was still very low after the short 7-days incubation (Figure S2, Figure S3).

3.4. N_2O, N_2 and CO_2 losses from soils of different erosion levels

3.4.1. CO_2 and total N_2O

Fluxes of CO_2 and total N_2Ot increased rapidly after the addition of fertilizer, reaching a maximum approximately 14 h after installation of the soil columns in the mesocosm facility (Fig. 2). Highest CO_2 losses right at the beginning of the experiment were found in columns that were filled only with topsoil material and planted with maize reaching mean values of 8.48 ± 0.92 mg C kg^{-1} d^{-1}. The peak in CO_2 fluxes decreased with increasing erosion level and in the treatments without maize, generally following the order E0p > E1p > E2p > E0 > E1 > E2 (Fig. 2). After 36 h, the CO_2 fluxes converged and remained almost constant for the rest of the incubation time in the non-planted columns. In the columns with maize, CO_2 fluxes showed a typical day-night pattern, after fluxes of the different soils have also been converged. In weakly and strongly eroded treatments, CO_2 fluxes exceeded initial maxima, reaching values of 10.73 ± 0.37 mg C kg^{-1} d^{-1} for E1p and 11.42 ± 1.30 mg C kg^{-1} d^{-1} for E2p, 75 h and 144 h after installation of the columns, respectively. We found maxima of N_2O fluxes at

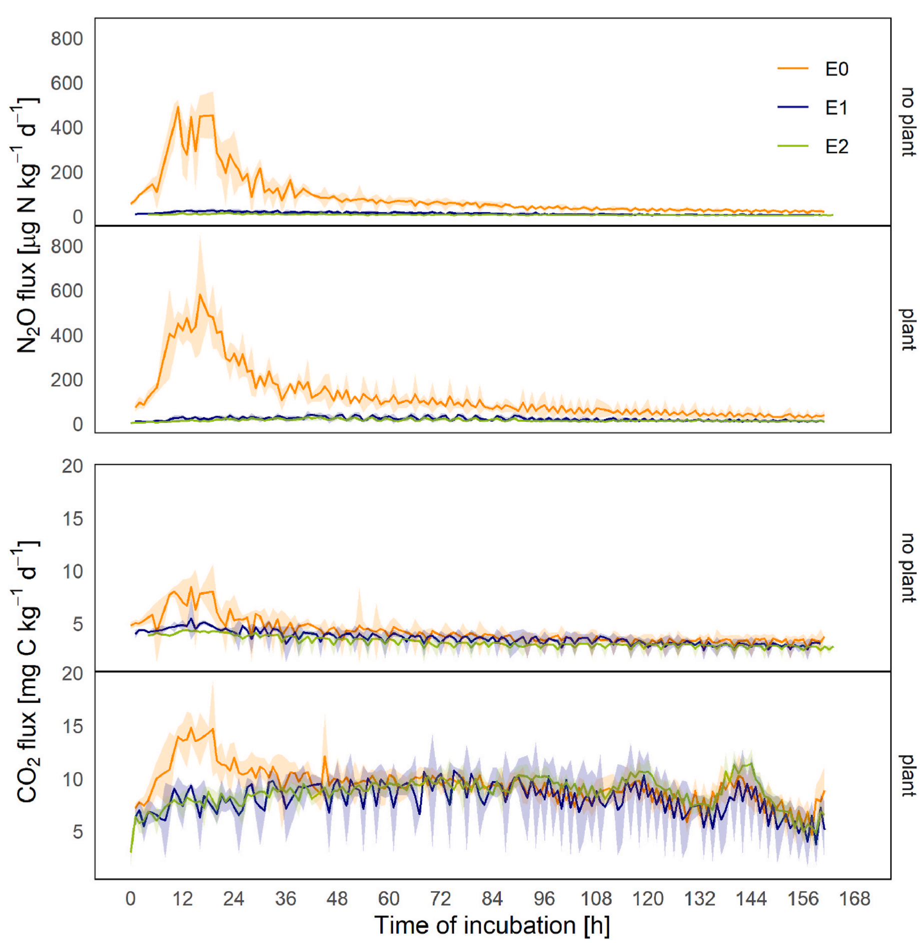

Figure 2. Mean N_2O and CO_2 fluxes over the 7-days incubation period of soils of different erosion levels (E0 = non eroded, E1 = weakly eroded, E2 = strongly eroded), planted with or without maize. Fluxes were measured continuously by GC. The number of observations decreased from n = 16 at the beginning to n = 4 at the end of the incubation, due to destructive soil sampling. Error bands represent ± standard deviation.

Table 4
Mean cumulative fluxes of CO_2 and total N_2O (N_2Ot), measured by GC, as well as N_2O and N_2 losses derived from the ^{15}N-labelled NO_3^- pool (fp_N_2O_{NO3}, fp_N_2), N_2O losses derived from non-labelled sources (fn_N_2O), and N_2O losses derived from the labelled $^{15}NH_4$ pool (fp_N_2O_{NH4}) for the $NH_4^{15}NO_3$ ($^{15}NO_3$) and the $^{15}NH_4NO_3$ ($^{15}NH_4$) treatment. Values represent treatment means ± standard deviation per treatment with n = 4. Different letters indicate significant differences between the studied erosion levels (E0 = non eroded, E1 = weakly eroded, E2 = strongly eroded) (capital letters) and treatments with (E0p, E1p, E2p) and without maize (E0, E1, E2) (lowercase letters) according to ANOVA followed by Tukey's HSD test ($p < 0.05$).

Treatment	tracer	total CO_2 [mg C kg^{-1} d^{-1}]	total N_2O (N_2Ot) [µg N kg^{-1} d^{-1}]	N_2O from NO_3 (fp_N_2O_{NO3}) [µg N kg^{-1} d^{-1}]	N_2O from NH_4 (fp_N_2O_{NH4}) [µg N kg^{-1} d^{-1}]	N_2O from other sources (fn_N_2O) [µg N kg^{-1} d^{-1}]	N_2 (fp_N_2) $^+$ [µg N kg^{-1} d^{-1}]	N_2Oi [-]
E0	$^{15}NO_3^-$	3.25 ± 0.96 a A	50.59 ± 23.22 a A	45.45 ± 21.54 a A	n.d.	5.14 ± 1.9 a A	23.81 ± 9.02 a A	0.64 ± 0.07 a A
E1	$^{15}NO_3^-$	2.58 ± 0.22 ab A	10.65 ± 7.18 b A	7.7 ± 6.22 b A	n.d.	2.95 ± 0.97 b A	15.09 ± 8.71 a A	0.33 ± 0.22 b A
E2	$^{15}NO_3^-$	2.22 ± 0.16 b A	2.54 ± 1.46 b A	0.95 ± 0.84 b A	n.d.	1.59 ± 0.62 b A	2.41 ± 1.55 b A	0.26 ± 0.08 b A
E0p	$^{15}NO_3^-$	8.81 ± 0.71 a B	79.49 ± 4.8 a B	73.27 ± 5.17 a B	n.d.	6.22 ± 0.62 a A	51.04 ± 8.35 a B	0.59 ± 0.04 a A
E1p	$^{15}NO_3^-$	4.66 ± 2.85 ab B	17.18 ± 12.52 b B	14.15 ± 10.58 b B	n.d.	3.03 ± 2.04 b A	52.62 ± 25.05 a B	0.19 ± 0.14 b A
E2p	$^{15}NO_3^-$	6.74 ± 1.12 b B	9.8 ± 1.44 b B	6.49 ± 1.35 b B	n.d.	3.32 ± 0.18 b A	21.12 ± 10.77 b B	0.25 ± 0.06 b A
E0	$^{15}NH_4^+$	3.44 ± 0.45 A	62.11 ± 16.98 a A	56.05 ± 15.47 a A	5.63 ± 1.42 a A	0.43 ± 0.18 a A	8.78 ± 3.29 a	n.d.
E1	$^{15}NH_4^+$	2.7 ± 0.22 A	7.11 ± 2.38 b A	4.62 ± 1.52 b A	1.26 ± 0.3 b A	1.24 ± 0.59 a A	13.95 ± 11.56 a	n.d.
E2	$^{15}NH_4^+$	2.24 ± 0.15 A	6.01 ± 4.34 b A	1.95 ± 1.38 b A	1.67 ± 1.56 b A	2.39 ± 1.41 a A	2.76 ± 0.7 a	n.d.
E0p	$^{15}NH_4^+$	7.6 ± 0.59 B	96.67 ± 44.42 a A	88.90 ± 40.75 a A	5.17 ± 0.67 a A	2.59 ± 4.27 a A	44.76 ± 21.13 b	n.d.
E1p	$^{15}NH_4^+$	7.07 ± 1.24 B	14.96 ± 5.95 b A	11.97 ± 4.79 b A	2.38 ± 1.01 b A	0.61 ± 0.28 a A	15.83 ± 7.3 a	n.d.
E2p	$^{15}NH_4^+$	6.8 ± 1.1 B	11.17 ± 4.89 b A	7.17 ± 3.1 b A	1.75 ± 0.89 b A	2.25 ± 1 a A	3.62 ± 1.27 a	n.d.

$^+$ Letters of the $^{15}NH_4^+$ treatment indicate significant differences for both treatments together to describe the significant interaction between the factors: erosion level and plant presence. n.d. = not determined.

comparable times to the CO_2 fluxes, with more pronounced differences observed between the different erosion levels than for CO_2 (Fig. 2). The N_2O fluxes remained almost constant throughout the incubation period. Lower emissions were observed in treatments E1, E1p, E2, and E2p, while notably higher fluxes were recorded in E0 and E0p.

Mean cumulative CO_2 losses over the short 7-day incubation period decreased slightly with increasing erosion level for the non-planted treatments, following the order E0 > E1 > E2 (Table 4). In the presence of maize, CO_2 losses increased significantly but followed a similar erosion-related trend to that observed in non-planted treatments. Total cumulative N_2O losses showed the same pattern observed for CO_2, with the highest emissions found in the non-eroded topsoils planted with maize (Table 4). The differences between erosion level E1 and E2 were less pronounced than the differences to the non-eroded control (E0). Overall, incorporating subsoil into topsoil reduced N_2O losses by over 80 % in both planted and non-planted treatments.

3.4.2. Source-related N_2O and N_2 losses

Analysis of isotopes enables us to distinguish N_2O losses stemming from the labelled NH_4^+ or NO_3^- pool through NH_4^+ oxidation or nitrifier denitrification, and denitrification, co-denitrification or coupled nitrification-denitrification, respectively. Additionally, N_2 losses, derived from the NO_3^- pool via denitrifying processes (s.a.) were calculated. In general, gaseous N losses from different sources decreased with increasing erosion level, in parallel with N_2Ot (Table 4). Fluxes of fp_N_2O_{NO3}, fp_N_2O_{NH4}, fn_N_2O and fp_N_2 over the entire 7-days

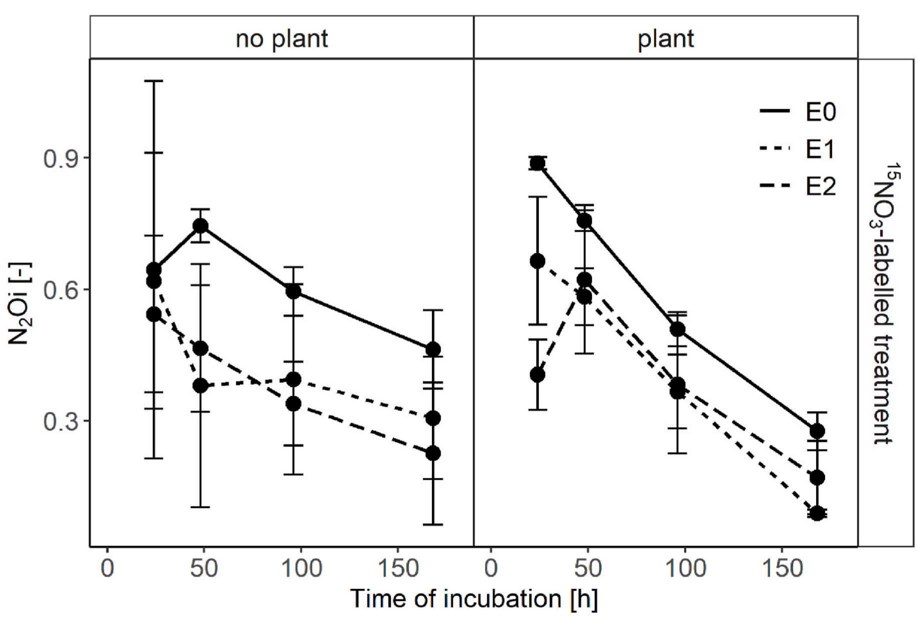

Figure 3. Mean N_2Oi ratio of denitrification over the 7-days incubation period from topsoils of different erosion levels (E0 = non eroded, E1 = weakly eroded, E2 = strongly eroded), planted with or without maize and after application of $NH_4^{15}NO_3$. Values represent treatment means ± standard deviation (n = 4).].

incubation can be found in the Supplementary (Figure S11 to Figure S14). The highest mean gaseous N fluxes were observed for E0p (Table 4). Total N_2O losses derived from the NO_3^- pool accounted for more than 90 % of total N_2O losses in these treatments. However, the proportion of N_2O from the NO_3^- pool decreased significantly with increasing erosion level, reaching minima of 32.42 % in the $^{15}NH_4$-labelled treatments and 37.38 % in the $^{15}NO_3$-labelled treatments, when topsoil was strongly eroded (E2) and maize plants were absent (Table 4). Values for fn_N_2O of the $^{15}NO_3$-labelled treatment showed the same trend with erosion level and were close to the fp_N_2O_{NH4} values of the $^{15}NH_4$-labelled treatments.

The N_2O losses derived from different soil N pools (fp_N_2O_{NO3}, fp_N_2O_{NH4}, fn_N_2O_{NH4}) significantly decreased when topsoil was diluted by subsoil material, irrespective of the erosion level and the applied fertilizer ($^{15}NH_4NO_3$, $NH_4^{15}NO_3$) (Table 4). In contrast the reduction in N_2 losses (fp_N_2) due to topsoil dilution was less pronounced in both ^{15}N treatments. In the $^{15}NO_3$-labelled treatments, differences in fp_N_2 from the non-eroded control (E0, E0p) were only significant for the strongly eroded topsoil (E2, E2p), where fp_N_2 was reduced by more than 50 %. In the $^{15}NH_4$-labelled treatments, a significant decrease of N_2 losses was only observed in planted treatments. Although N_2 losses decline with erosion level also in the treatments without maize, differences were not significant.

The presence of maize plants generally increased gaseous N losses from different sources, regardless of the erosion level. However, these differences were only significant for N_2Ot, fp_N_2O, fp_N_2 in the $^{15}NO_3$-labelled treatments, but not in the $^{15}NH_4$-labelled treatments. In general, no interaction between the two studied factors, erosion level and plant presence were found, except for fp_N_2 in the NH_4-labelled treatments.

Values for N_2Oi were only calculated for $^{15}NO_3$-labelled treatments with maxima corresponding to highest total N_2O losses at the beginning of the experiment. Therefore, N_2Oi decreased significantly with erosion level, with highest values observed for the non-eroded topsoils with values of 0.89 ± 0.01 for E0p and 0.64 ± 0.43 for E0 after 24 h of incubation (Fig. 3). N_2Oi also decreased with time, reaching a minimum after 168 h of incubation. Overall, topsoil erosion had a significant effect on N_2Oi irrespective of maize presence (Table 4).

Differences between the different tracers ($^{15}NH_4NO_3$, $NH_4^{15}NO_3$) were only marginal and resulted from different calculation procedures of the same value (see section 2.5.1.).

4. Discussion

4.1. Impact of topsoil erosion levels on gross N transformation rates

Gross N transformation rates were generally within the range reported in other studies that modeled rates in the field (Holz et al., 2016; Laine et al., 2018) or in the laboratory (Rütting and Müller, 2007; Inselsbacher et al., 2013; Castellano-Hinojosa et al., 2020; He et al., 2020; Lama et al., 2020) using *Ntrace*. Oxidation of NH_4^+ to NO_3^- was the dominant process across all topsoils, regardless of erosion level or plant presence. This was expected, considering that NH_4^+ is the main limiting factor for gross NH_4^+ oxidation rates in agricultural soils (Booth et al., 2005; Robertson and Groffman, 2015; Norton and Ouyang, 2019) and that in our setup high amounts of NH_4^+-N were added with the fertilizer. Differences in gross NH_4^+ oxidation rates between the two eroded topsoils (E1, E2) and the non-eroded control (E0) were consistent with the differences in NH_4^+ contents after the addition of fertilizer. This indicates that substrate availability, rather than microbial abundance, reduced gross NH_4^+ oxidation rates as the level of erosion increased.

N transformation pathways requiring organic sources, were undetectable in any of the soil treatments (e.g. DNRA, N_{org} oxidation to NO_3^-). Gross N mineralization rates indicated that the absence of these pathways was due to limitations in organic matter, as reflected by total organic C contents. The availability of organic C and N for microbes in eroded compared to non-eroded topsoil can further be reduced by the more recalcitrant nature of organic matter in subsoils (Schrumpf et al., 2013; Jones et al., 2018), and the fact that it can be stabilized in subsoil by free mineral particles (Harden et al., 1999; Baldock and Skjemstad, 2000; Doetterl et al., 2016). Differences in microbial structure and abundance between subsoil and topsoil can further affect N transformation processes in eroded topsoils, whereby changes would be more associated with changes in C_{org} content in our experiment than other soil properties, such as soil pH. Jones et al. (2018) found an exponential decrease in N mineralization rates with increasing soil depth, corresponding to lower microbial biomass in subsoil compared to the topsoil.

Although N_t contents and ^{15}N abundances increased in plant biomass throughout the incubation (Figure S2, Figure S3), we were unable to simulate plant NH_4^+ and NO_3^- uptake using the *Ntrace* model. We assume that this is due to N contributions from caryopses of the young maize plants (Watt and Cresswell, 1987), which likely biased our simulations. In total, only 5 % of the applied ^{15}N fertilizer was recovered in plant biomass. However, plants can stimulate microbial activity even at early growth stages, when C-rich photosynthates are released into the soil via root exudates, which increases microbial growth and, consequently, microbial N turnover (Herman et al., 2006; Kuzyakov and Xu, 2013; Finzi et al., 2015; He et al., 2020; Holz et al., 2023). Therefore, we assumed that the reduction in organic matter by topsoil dilution can be partly counterbalanced by plant presence. This was only partly confirmed by the significantly higher gross N mineralization rates in E2p treatments compared to the rates measured in E1, E2 and E1p.

4.2. Impact of topsoil erosion levels on CO_2, N_2O and N_2 losses from different N pools

4.2.1. CO_2 losses

Our results indicate that both erosion level and the presence of plants considerably affected CO_2 losses. Elevated CO_2 emissions at the start of incubation resulted from heterotrophic respiration, which was promoted by physical soil disturbance and associated aeration of the soil material (Roberts and Chan, 1990; Reicosky, 1997; Chatskikh and Olesen, 2007; Smith et al., 2007; Sainju et al., 2012). The CO_2 losses in this experiment were slightly higher compared to Senbayram et al. (2009), who reported a maximum between 0.49 mg C kg^{-1} d^{-1} and 1.09 mg C kg^{-1} d^{-1} after ammonium sulphate application. This can be explained by higher soil water contents in their experiment, favoring anoxic conditions and, hence, impeding soil respiration. Soil water contents in the range of 40 %–70 % WFPS are known to represent optimal conditions for soil respiration (Linn and Doran, 1984; Gritsch et al., 2015). Furthermore, the addition of N with the fertilizer may have increased microbial activity and growth in general, enhancing CO_2 losses from heterotrophic respiration (Lu et al., 2011; Robertson and Groffman, 2015). Plants additionally influence CO_2 losses via autotrophic respiration (Kuzyakov, 2006), which was shown in significantly higher cumulative CO_2 losses at the end of the 7-days incubation.

Overall, the observed decrease of CO_2 emissions with increasing erosion levels is in accordance with other studies, reporting lower CO_2 losses in eroded soils (Reicosky et al., 2005; Gao et al., 2020; Vaidya et al., 2024). In contrast to gross N mineralization rates, cumulative CO_2 losses decline directly proportional to the reduction in C_{org} content, supporting our hypothesis that microbial activity is mainly restricted by C availability in eroded topsoils. Differences in CO_2 emissions between different erosion levels were less pronounced throughout the incubation period than during the initial 0–48 h, even in unplanted treatments, indicating a slower microbial response to fertilization and soil mixing. This is in accordance with Jones et al. (2018), who found that the addition of organic C and N increased microbial C and N turnover in both topsoil and subsoil, but the response in subsoil was notably delayed. We assume that lower microbial activity at the beginning of the incubation, but primarily limited organic C availability, restricted C and N turnover in eroded topsoils compared to the non-eroded controls.

4.2.2. N_2O and N_2 losses

For the first time, we could show that not only N_2O fluxes, but also N_2 losses decrease in eroded compared to non-eroded topsoils in treatments with and without maize, supporting our hypothesis that N_2O and N_2 losses decrease with topsoil dilution. Measured N_2O and N_2 losses were in the range of values published by Buchen-Tschiskale et al. (2020) who reported cumulative fluxes between 7.30 and 44.44 μg N kg^{-1} d^{-1} for N_2O and between 9.65 and 58 0.57 μg N kg^{-1} d^{-1} for N_2 in a short-term incubation experiment using arable soils with similar properties after application of calcium ammonium nitrate (CAN). However, $N_2O + N_2$ losses were relatively low compared to other incubation studies, measuring denitrification losses following mineral fertilizer application (Mulvaney et al., 1997; Hütsch et al., 1999; Senbayram et al., 2020). This could be explained by differences in water content, which is known to significantly affect N_2O and N_2 production (Firestone and Davidson, 1989). High water contents of >60 % WFPS are known to substantially increase $N_2O + N_2$ production via denitrification compared to soils with lower soil water contents (Ruser et al., 2006; Gu et al., 2011; Butterbach-Bahl et al., 2013).

The *Ntrace* model results in this experiment showed the highest rates of N turnover via NH_4^+ oxidation to NO_3^-, indicating that N_2O losses derived mainly from the soil NH_4^+ pool and, hence, from NH_4^+ and NO_2^- oxidation, nitrifier denitrification or coupled nitrification denitrification. Nitrifier denitrification includes the oxidation of NH_4^+ to intermediates such as NO_2^-, followed by its reduction to N_2O and N_2 and has long been underestimated as N_2O source in soils (Wrage et al., 2001; Wrage-Mönnig et al., 2018). Several authors have shown that nitrifier denitrification can produce substantial amounts of N_2O, accounting for up to 90 % of total N_2O emissions, as summarized by Wrage-Mönnig et al. (2018). This is particularly true for soils under low O_2 conditions (Zhu et al., 2013) and reduced SOC levels (Mooshammer et al., 2014). Unlike heterotrophic bacterial denitrification, where NO_3^- serves as the substrate for N_2O production, nitrifier denitrification directly generates N_2O after NH_4^+ oxidation to NO_2^- (Wrage et al., 2001). In this experiment, however, the isotopic signature of produced N_2O indicated that most of it was derived from the soil NO_3^- pool and, therefore, from denitrification. In the non-eroded topsoils less than 10 % of the N_2O originated from the NH_4^+ pool, although water contents generally favor aerobic soil conditions (40 % WFPS). This contradicts findings in Bateman and Baggs (2005), who observed that more than 80 % of the measured N_2O came from oxidation of NH_4^+ at soil water contents between 35 and 60 % WFPS. We assume that NH_4^+ oxidation to NO_3^-, promoted by NH_4^+ application and an optimal water as well as O_2 supply, created anaerobic zones in the soils of this experiment, enabling denitrification to occur (Azam et al., 2002; O'Neill et al., 2020). This process is referred to as coupled nitrification denitrification and is known to occur if conditions are neither optimal for nitrification nor for denitrification (Wrage et al., 2001). This is supported by the results from the *Ntrace* model, which showed highest N turnover via NH_4^+ oxidation to NO_3^-. Furthermore, N_2Oi ratios showed that more than 50 % of gaseous N losses from the NO_3^- pool occurred in the form of N_2O, indicating that denitrification was incomplete. Incomplete denitrification refers to the phenomena that NO_3^- is reduced only to N_2O, as the N_2O reductase, which further reduces N_2O to N_2, is more strongly inhibited by the presence of O_2 than the N_2O producing reductases (Knowles, 1982; Baggs, 2011). This is especially true for soils containing high amounts of NO_3^- as electron acceptors, as in our experiment (Robertson and Tiedje, 1987; Bremner, 1997; Senbayram et al., 2019). Emissions of N_2O can also occur through dissimilatory nitrate reduction to ammonium (DNRA), which requires conditions similar to heterotrophic denitrification (Tiedje et al., 1982; Rütting et al., 2011a; Putz et al., 2018). However, as the $^{15}NO_3$-labelled treatments showed no ^{15}N flux from the NO_3^- pool to the non-labelled NH_4^+ pool at any time during the incubation, DNRA was assumed not to occur. This was further confirmed by the model results of *Ntrace*.

Increased N_2O production was particularly evident in the non-eroded treatment, where emissions were highest and N_2Oi showed maximum values of almost 0.90. Microorganisms capable of reducing NO_3^- are ubiquitous throughout the soil profile (McCarty and Bremner, 1992). Hence, it is unlikely that the dilution of topsoil in this experiment reduced the denitrifier community. However, denitrification in soils with high NO_3^- and low O_2 contents is mainly limited by SOC availability (Burford and Bremner, 1975; Bremner, 1997). A lower SOC availability in the eroded topsoils might, therefore, be the main reason for the substantial lower N_2O and N_2 losses in eroded topsoils compared to the non-eroded control. On the one hand, SOC serves as an electron donor for heterotrophic denitrifying organisms; on the other hand, the amount of SOC determines soil respiration and, thus, the consumption and depletion of O_2 (Buchen-Tschiskale et al., 2023; Robertson and Groffman, 2024). As CO_2 fluxes peaked with the N_2O fluxes in this experiment, we assume that O_2 depletion was the main limiting factor controlling denitrification in this experiment immediately after aeration and fertilization. Furthermore, gross rates of N mineralization to NH_4^+ as well as NH_4^+ immobilization were substantially lower in the eroded topsoils (E1, E2) compared to the control treatment (E0), indicating lower microbial activity and lower respiration.

In addition to N_2O, NO can be produced through various biotic and abiotic processes, such as NH_4^+ oxidation, heterotrophic nitrification, heterotrophic denitrification, chemodenitrification or nitrifier denitrification (Medinets et al., 2015 and references therein). While N_2O is predominately associated with denitrification under high soil water moisture, the proportion of NO losses on total N_2O + NO is considered to increase under conditions favoring NH_4^+ oxidation (Ludwig et al., 2001; Zhu et al., 2013; Russow et al., 2008). Given that oxidation of NH_4^+ dominating N cycling, NO emissions could represent a relevant N loss pathway in this experiment.

Treatments with maize increased the production of N_2O and N_2 compared to non-planted treatments by factors of 2.1 and 2.6, respectively. This is in line with Yankelzon et al. (2024), who reported 4-fold higher N_2O and 1.8-fold higher N_2 losses in planted compared to non-planted treatments. Similarly, an experiment with barley conducted by Senbayram et al. (2020) showed a 3-fold increase in N_2O and N_2 emissions, but no effect on the N_2Oi ratios. Microbial activity is generally known to be stimulated in the rhizosphere due to root exudation, releasing nutrients, sugars and amino acids to the soil (Ma et al., 2022). Hence, roots provide an additional organic C source for microbes, accelerating soil C and N turnover and the decomposition of SOM (Herman et al., 2006; Finzi et al., 2015; Holz et al., 2023). Apart from stimulating microbial activity after mixing and fertilization right at the beginning of the incubation, plant presence likely increased the release of N_2O and N_2 from soils over the entire incubation time in this experiment. Due to the small age of the plants and the short incubation time, plants were probably not strongly competing with microbes for N (Kuzyakov and Xu, 2013) and consequently NO_3^- availability was probably not limiting microbes. A limitation of the denitrification source was only shown to occur in longer experiments. For example, Rummel et al. (2021) reported reduced N_2O and N_2 losses from denitrification with higher plant N and water uptake, attributed to lower NO_3^- availability for microbes. In contrast to our assumption, plant presence did not counterbalance the effect of erosion-induced topsoil dilution on gaseous formation of $N_2O + N_2$. As plants were at a young growth stage, their N uptake was still on a low level, as was its effect on N transformations such as denitrification.

4.3. Impact of topsoil erosion levels on plant N uptake

We hypothesized that fertilizer N uptake (Ndff) increases with increasing erosion level, due to lower inherent N contents in eroded topsoils. This was partly confirmed in this experiment, where significant differences between erosion levels were observed only in the strongly eroded soils of the $^{15}NO_3$-labelled treatments. Pradhan et al. (1997) investigated the effect of erosion depth on fertilizer N uptake in artificially eroded soils. They found that reduced N mineralization in the subsoil led to greater plant uptake of fertilizer N. This aligns with our results that showed increased Ndff values with increasing erosion level and further supports our hypothesis that plants had less soil-borne N available and, therefore, took up N mainly from fertilizer. Malhi et al. (2004) also observed higher Ndff values in upper slope positions with truncated topsoil compared to lower slope positions, which is consistent with the results of this study. At the same time, they found less of the applied fertilizer-^{15}N in the plant material in eroded soils, indicating lower N uptake in general from the eroded soils. To verify our hypothesis, future investigations should consider plant N uptake throughout the entire growing season. The experimental setup in this study did not allow for a longer incubation period, as it was designed to prevent reflux of applied ^{15}N into the source N pool.

5. Conclusion

Topsoil erosion reduced C_{org} and N_t contents with increasing erosion level, leading to a simultaneous decline in gross N transformation rates. Oxidation of NH_4^+ to NO_3^- was by far the dominating N pathway across all investigated topsoils, promoted mainly by the addition of the NH_4^+-based fertilizer. Differences in denitrification rates further indicate that soil organic C was the main limiting factor for heterotrophic N turnover pathways. This was also reflected in the low mineralization rates compared to other studies. However, besides denitrification, only three processes significantly affected N cycling (NH_4^+ oxidation > N_{org} mineralization > NH_4^+ immobilization), as demonstrated by the results of the *Ntrace* model. Simulation of plant N uptake was impossible at the young growth stages of the maize, but plants, however, affected gross N transformation rates positively.

Due to lower nitrification and denitrification rates, topsoil dilution also significantly reduced N losses via N_2O and N_2 from various sources, independent of maize presence. However, plants significantly affected gaseous N losses, probably by providing an additional C source through root exudation even at very young growth stages. Although, we found a trend of increasing Ndff with erosion level, experiments need to be transferred to the field to understand how N fluxes are affected throughout the entire season. Additionally, combining presented approaches with methods to investigate microbial communities in this context would be crucial to further improve our process understanding. Furthermore, other soil types formed by erosion in hilly terrain should also be focused, e.g. at depositional positions known to be C-enriched. Moreover, this study provides unique quantitative data on N fluxes, including N_2O and N_2 emissions, in eroded soils, which can be used as a valuable basis for further model development.

CRediT authorship contribution statement

Julia Schoof: Writing – review & editing, Writing – original draft, Visualization, Validation, Methodology, Investigation, Data curation, Conceptualization. **Maire Holz:** Writing – review & editing, Validation, Supervision, Resources, Project administration, Methodology, Funding acquisition, Conceptualization. **Tobias Rütting:** Writing – review & editing, Validation, Software, Methodology. **Reinhard Well:** Writing – review & editing, Validation, Software, Methodology. **Caroline Buchen-Tschiskale:** Writing – review & editing, Validation, Supervision, Resources, Project administration, Methodology, Investigation, Funding acquisition, Conceptualization.

Declaration of competing interest

The authors declare that they have no known competing financial interests or personal relationships that could have appeared to influence the work reported in this paper.

Acknowledgements

This study was supported by the German Research Foundation (DFG BU 3719/3-1 and HO 6381/4-1). Many thanks are due to Michael Sommer for supplying soil; Stefan Burkart and Carina Wittke for help in the mesocosm facility; Martina Heuer and Ute Rieβ for isotopic analysis; Nicole Altwein, Ute Tambor and Claudia Wiese for soil analysis; Lea Siebelt for help with sample preparation and Jens Dyckmans and his team for SPIN-MIRMS analysis.

Appendix A. Supplementary data

Supplementary data to this article can be found online at https://doi.org/10.1016/j.soilbio.2025.109905.

References

Allmaras, R.R., Burwell, R.E., Holt, R.F., 1967. Plow-layer porosity and surface roughness from tillage as affected by initial porosity and soil moisture at tillage time. Soil Science Society of America Journal 31, 550–556. https://doi.org/10.2136/sssaj1967.03615995003100040033x.

Azam, F., Müller, C., Weiske, A., Benckiser, G., Ottow, J.C.G., 2002. Nitrification and denitrification as sources of atmospheric nitrous oxide - role of oxidizable carbon and applied nitrogen. Biology and Fertility of Soils 35, 54–61. https://doi.org/10.1007/s00374-001-0441-5.

Baggs, E.M., 2011. Soil microbial sources of nitrous oxide: recent advances in knowledge, emerging challenges and future direction. Current Opinion in Environmental Sustainability 3, 321–327. https://doi.org/10.1016/j.cosust.2011.08.011.

Baldock, J.A., Skjemstad, J.O., 2000. Role of the soil matrix and minerals in protecting natural organic materials against biological attack. Organic Geochemistry 31, 697–710. https://doi.org/10.1016/s0146-6380(00)00049-8.

Barraclough, D., 1995. ^{15}N isotope dilution techniques to study soil nitrogen transformations and plant uptake. Fertilizer Research 42, 185–192. https://doi.org/10.1007/bf00750513.

Bateman, E.J., Baggs, E.M., 2005. Contributions of nitrification and denitrification to N_2O emissions from soils at different water-filled pore space. Biology and Fertility of Soils 41, 379–388. https://doi.org/10.1007/s00374-005-0858-3.

Bergsma, T.T., Ostrom, N.E., Emmons, M., Robertson, G.P., 2001. Measuring simultaneous fluxes from soil of N_2O and N_2 in the field using the ^{15}N-gas "nonequilibrium" technique. Environmental Science & Technology 35, 4307–4312. https://doi.org/10.1021/es010885u.

Berhe, A.A., Barnes, R.T., Six, J., Marín-Spiotta, E., 2018. Role of soil erosion in biogeochemical cycling of essential elements: carbon, nitrogen, and phosphorus. Annual Review of Earth and Planetary Sciences 46, 521–548. https://doi.org/10.1146/annurev-earth-082517-010018.

Berhe, A.A., Harden, J.W., Torn, M.S., Kleber, M., Burton, S.D., Harte, J., 2012. Persistence of soil organic matter in eroding versus depositional landform positions. Journal of Geophysical Research: Biogeosciences 117. https://doi.org/10.1029/2011jg001790.

Berhe, A.A., Torn, M.S., 2017. Erosional redistribution of topsoil controls soil nitrogen dynamics. Biogeochemistry 132, 37–54. https://doi.org/10.1007/s10533-016-0286-5.

Booth, M.S., Stark, J.M., Rastetter, E., 2005. Controls on nitrogen cycling in terrestrial ecosystems: a synthetic analysis of literature data. Ecological Monographs 75, 139–157. https://doi.org/10.1890/04-0988.

Borrelli, P., Panagos, P., Alewell, C., Ballabio, C., de Oliveira Fagundes, H., Haregeweyn, N., Lugato, E., Maerker, M., Poesen, J., Vanmaercke, M., Robinson, D. A., 2022. Policy implications of multiple concurrent soil erosion processes in European farmland. Nature Sustainability 6, 103–112. https://doi.org/10.1038/s41893-022-00988-4.

Bremner, J.M., 1997. Sources of nitrous oxide in soils. Nutrient Cycling in Agroecosystems 49, 7–16. https://doi.org/10.1023/a:1009798022569.

Buchen-Tschiskale, C., Hagemann, U., Augustin, J., 2020. Soil incubation study showed biogas digestate to cause higher and more variable short-term N_2O and N_2 fluxes than mineral-N. Journal of Plant Nutrition and Soil Science 183, 208–219. https://doi.org/10.1002/jpln.201900075.

Buchen-Tschiskale, C., Well, R., Flessa, H., 2023. Tracing nitrogen transformations during spring development of winter wheat induced by ^{15}N labeled cattle slurry applied with different techniques. Sci Total Environ 871, 162061. https://doi.org/10.1016/j.scitotenv.2023.162061.

Buchen, C., Lewicka-Szczebak, D., Fuß, R., Helfrich, M., Flessa, H., Well, R., 2016. Fluxes of N_2 and N_2O and contributing processes in summer after grassland renewal and grassland conversion to maize cropping on a Plaggic Anthrosol and a Histic Gleysol. Soil Biology and Biochemistry 101, 6–19. https://doi.org/10.1016/j.soilbio.2016.06.028.

Burford, J.R., Bremner, J.M., 1975. Relationships between the denitrification capacities of soils and total, water-soluble and readily decomposable soil organic matter. Soil Biology and Biochemistry 7, 389–394. https://doi.org/10.1016/0038-0717(75)90055-3.

Butterbach-Bahl, K., Baggs, E.M., Dannenmann, M., Kiese, R., Zechmeister-Boltenstern, S., 2013. Nitrous oxide emissions from soils: how well do we understand the processes and their controls? Philosophical Transactions of the Royal Society of London B Biological Sciences 368, 20130122. https://doi.org/10.1098/rstb.2013.0122.

Castellano-Hinojosa, A., Charteris, A.F., Müller, C., Jansen-Willems, A., González-López, J., Bedmar, E.J., Carrillo, P., Cárdenas, L.M., 2020. Occurrence and ^{15}N-quantification of simultaneous nitrification and denitrification in N-fertilised soils incubated under oxygen-limiting conditions. Soil Biology and Biochemistry 143. https://doi.org/10.1016/j.soilbio.2020.107757.

Castellano, M.J., Kaye, J.P., Lin, H., Schmidt, J.P., 2012. Linking carbon saturation concepts to nitrogen saturation and retention. Ecosystems 15, 175–187. https://doi.org/10.1007/s10021-011-9501-3.

Chatskikh, D., Olesen, J.E., 2007. Soil tillage enhanced CO_2 and N_2O emissions from loamy sand soil under spring barley. Soil and Tillage Research 97, 5–18. https://doi.org/10.1016/j.still.2007.08.004.

Chen, Z., Ding, W., Xu, Y., Müller, C., Rütting, T., Yu, H., Fan, J., Zhang, J., Zhu, T., 2015. Importance of heterotrophic nitrification and dissimilatory nitrate reduction to ammonium in a cropland soil: evidences from a ^{15}N tracing study to literature synthesis. Soil Biology and Biochemistry 91, 65–75. https://doi.org/10.1016/j.soilbio.2015.08.026.

Daims, H., Lücker, S., Wagner, M., 2016. A new perspective on microbes formerly known as nitrite-oxidizing bacteria. Trends in Microbiology 24, 699–712. https://doi.org/10.1016/j.tim.2016.05.004.

Davidson, E.A., Hart, S.C., Shanks, C.A., Firestone, M.K., 1991. Measuring gross nitrogen mineralization, immobilization, and nitrification by ^{15}N isotopic pool dilution in intact soil cores. European Journal of Soil Science 42, 335–349. https://doi.org/10.1111/j.1365-2389.1991.tb00413.x.

Doetterl, S., Berhe, A.A., Nadeu, E., Wang, Z., Sommer, M., Fiener, P., 2016. Erosion, deposition and soil carbon: a review of process-level controls, experimental tools and models to address C cycling in dynamic landscapes. Earth-Science Reviews 154, 102–122. https://doi.org/10.1016/j.earscirev.2015.12.005.

Doran, J.W., 1987. Microbial biomass and mineralizable nitrogen distributions in no-tillage and plowed soils. Biology and Fertility of Soils 5. https://doi.org/10.1007/bf00264349.

Dyckmans, J., Eschenbach, W., Langel, R., Szwec, L., Well, R., 2021. Nitrogen isotope analysis of aqueous ammonium and nitrate by membrane inlet isotope ratio mass spectrometry (MIRMS) at natural abundance levels. Rapid Communications in Mass Spectrometry 35, e9077. https://doi.org/10.1002/rcm.9077.

Finzi, A.C., Abramoff, R.Z., Spiller, K.S., Brzostek, E.R., Darby, B.A., Kramer, M.A., Phillips, R.P., 2015. Rhizosphere processes are quantitatively important components of terrestrial carbon and nutrient cycles. Global Change Biology 21, 2082–2094. https://doi.org/10.1111/gcb.12816.

Firestone, M.K., Davidson, E.A., 1989. Microbiological basis of NO and N_2O production and consumption in soil. In: Andreae, M.O., Schimel, D.S. (Eds.), Exchange of Trace Gases between Terrestrial Ecosystems and the Atmosphere. Wiley & Sons, New York.

Fox, J., Weisberg, S., 2019. An R Companion to Applied Regression, 3 ed. Sage.

Galloway, J.N., Townsend, A.R., Erisman, J.W., Bekunda, M., Cai, Z., Freney, J.R., Martinelli, L.A., Seitzinger, S.P., Sutton, M.A., 2008. Transformation of the nitrogen cycle: recent trends, questions, and potential solutions. Science 320, 889–892. https://doi.org/10.1126/science.1136674.

Gao, X., Li, W., Salman, A., Wang, R., Du, L., Yao, L., Hu, Y., Guo, S., 2020. Impact of topsoil removal on soil CO_2 emission and temperature sensitivity in Chinese Loess Plateau. Science of The Total Environment 708. https://doi.org/10.1016/j.scitotenv.2019.135102.

Ghotbi, M., Taghizadeh-Mehrjardi, R., Knief, C., Ghotbi, M., Kent, A.D., Horwath, W.R., 2023. The patchiness of soil ^{13}C versus the uniformity of ^{15}N distribution with geomorphic position provides evidence of erosion and accelerated organic matter turnover. Agriculture, Ecosystems & Environment 356. https://doi.org/10.1016/j.agee.2023.108616.

Govers, G., Vandaele, K., Desmet, P., Poesen, J., Bunte, K., 1994. The role of tillage in soil redistribution on hillslopes. European Journal of Soil Science 45, 469–478. https://doi.org/10.1111/j.1365-2389.1994.tb00532.x.

Govindasamy, P., Muthusamy, S.K., Bagavathiannan, M., Mowrer, J., Jagannadham, P.T.K., Maity, A., Halli, H.M., K, S.G., Vadivel, R., T D, K., Raj, R., Pooniya, V., Babu, S., Rathore, S.S., L, M., Tiwari, G., 2023. Nitrogen use efficiency - a key to enhance crop productivity under a changing climate. Frontiers in Plant Science 14. https://doi.org/10.3389/fpls.2023.1121073.

Gritsch, C., Zimmermann, M., Zechmeister-Boltenstern, S., 2015. Interdependencies between temperature and moisture sensitivities of CO_2 emissions in European land ecosystems. Biogeosciences Discuss 12, 4433–4464. https://doi.org/10.5194/bgd-12-4433-2015.

Gu, J., Nicoullaud, B., Rochette, P., Pennock, D.J., Henault, C., Cellier, P., Richard, G., 2011. Effect of topography on nitrous oxide emissions from winter wheat fields in Central France. Environ Pollut 159, 3149–3155. https://doi.org/10.1016/j.envpol.2011.04.009.

Han, Z., Walter, M.T., Drinkwater, L.E., 2017. Impact of cover cropping and landscape positions on nitrous oxide emissions in northeastern US agroecosystems. Agriculture, Ecosystems & Environment 245, 124–134. https://doi.org/10.1016/j.agee.2017.05.018.

Harden, J.W., Sharpe, J.M., Parton, W.J., Ojima, D.S., Fries, T.L., Huntington, T.G., Dabney, S.M., 1999. Dynamic replacement and loss of soil carbon on eroding cropland. Global Biogeochemical Cycles 13, 885–901. https://doi.org/10.1029/1999gb900061.

Harris, E., Joss, A., Emmenegger, L., Kipf, M., Wolf, B., Mohn, J., Wunderlin, P., 2015. Isotopic evidence for nitrous oxide production pathways in a partial nitritation-anammox reactor. Water Research 83, 258–270. https://doi.org/10.1016/j.watres.2015.06.040.

He, X., Chi, Q., Cai, Z., Cheng, Y., Zhang, J., Müller, C., 2020. ^{15}N tracing studies including plant N uptake processes provide new insights on gross N transformations in soil-plant systems. Soil Biology and Biochemistry 141. https://doi.org/10.1016/j.soilbio.2019.107666.

Heckrath, G., Djurhuus, J., Quine, T.A., Van Oost, K., Govers, G., Zhang, Y., 2005. Tillage erosion and its effect on soil properties and crop yield in Denmark. Journal of Environmental Quality 34, 312–324. https://doi.org/10.2134/jeq2005.0312a.

Heil, J., Vereecken, H., Brüggemann, N., 2015. A review of chemical reactions of nitrification intermediates and their role in nitrogen cycling and nitrogen trace gas formation in soil. European Journal of Soil Science 67, 23–39. https://doi.org/10.1111/ejss.12306.

Herman, D.J., Johnson, K.K., Jaeger, C.H., Schwartz, E., Firestone, M.K., 2006. Root influence on nitrogen mineralization and nitrification in avena barbata rhizosphere soil. Soil Science Society of America Journal 70, 1504–1511. https://doi.org/10.2136/sssaj2005.0113.

Hoffmann, M., Pohl, M., Jurisch, N., Prescher, A.K., Mendez Campa, E., Hagemann, U., Remus, R., Verch, G., Sommer, M., Augustin, J., 2018. Maize carbon dynamics are driven by soil erosion state and plant phenology rather than nitrogen fertilization form. Soil and Tillage Research 175, 255–266. https://doi.org/10.1016/j.still.2017.09.004.

Holz, M., Augustin, J., 2021. Erosion effects on soil carbon and nitrogen dynamics on cultivated slopes: a meta-analysis. Geoderma 397. https://doi.org/10.1016/j.geoderma.2021.115045.

Holz, M., Aurangojeb, M., Kasimir, Å., Boeckx, P., Kuzyakov, Y., Klemedtsson, L., Rütting, T., 2016. Gross nitrogen dynamics in the mycorrhizosphere of an organic forest soil. Ecosystems 19, 284–295. https://doi.org/10.1007/s10021-015-9931-4.

Holz, M., Paterson, E., Pausch, J., 2023. Rhizosphere carbon priming: a plant mechanism to enhance soil nitrogen accessibility? Plant and Soil 488, 175–185. https://doi.org/10.1007/s11104-023-05979-8.

Hütsch, B.W., Wang, X., Feng, K., Yan, F., Schubert, S., 1999. Nitrous oxide emission as affected by changes in soil water content and nitrogen fertilization. Journal of Plant Nutrition and Soil Science 162, 607–613. https://doi.org/10.1002/(sici)1522-2624(199912)162:6<607::Aid-jpln607>3.0.Co;2-0.

IAEA, 1983. A Guide to the Use of Nitrogen-15 and Radioisotopes in Studies of Plant Nutrition: Calculations and Interpretation of Data. International Atmoic Energy Agency, Vienna, p. 65.

Inselsbacher, E., Wanek, W., Strauss, J., Zechmeister-Boltenstern, S., Müller, C., 2013. A novel ^{15}N tracer model reveals: plant nitrate uptake governs nitrogen transformation rates in agricultural soils. Soil Biology and Biochemistry 57, 301–310. https://doi.org/10.1016/j.soilbio.2012.10.010.

ISO, 2005. Soil Quality - Determination of Nitrate, Nitrite and Ammonium in Field Moist Soils by Extraction with Potassium Chloride Solution, Part 2: Automated Method with Segmented Flow Analysis. International Organization for Standardization, Switzerland.

IUSS Working Group, 2015. World Reference Base for Soil Resources 2014, Update 2015. International Soil Classification System for Naming Soils and Creating Legends for Soil Maps. FAO, Rome.

Jones, D.L., Magthab, E.A., Gleeson, D.B., Hill, P.W., Sánchez-Rodríguez, A.R., Roberts, P., Ge, T., Murphy, D.V., 2018. Microbial competition for nitrogen and carbon is as intense in the subsoil as in the topsoil. Soil Biology and Biochemistry 117, 72–82. https://doi.org/10.1016/j.soilbio.2017.10.024.

Kemmann, B., Ruf, T., Matson, A., Well, R., 2023. Waterlogging effects on N_2O and N_2 emissions from a Stagnosol cultivated with Silphium perfoliatum and silage maize. Biology and Fertility of Soils 59, 53–71. https://doi.org/10.1007/s00374-022-01673-6.

Kemmann, B., Wöhl, L., Fuß, R., Schrader, S., Well, R., Ruf, T., 2021. N_2 and N_2O mitigation potential of replacing maize with the perennial biomass crop Silphium perfoliatum - an incubation study. GCB Bioenergy 13, 1649–1665. https://doi.org/10.1111/gcbb.12879.

Khalil, K., Mary, B., Renault, P., 2004. Nitrous oxide production by nitrification and denitrification in soil aggregates as affected by O_2 concentration. Soil Biology and Biochemistry 36, 687–699. https://doi.org/10.1016/j.soilbio.2004.01.004.

Kirkham, D., Bartholomew, W.V., 1954. Equations for following nutrient transformations in soil, utilizing tracer Data1. Soil Science Society of America Journal 18. https://doi.org/10.2136/sssaj1954.03615995001800010009x.

Knowles, R., 1982. Denitrification. Microbiological Reviews 46, 43–70. https://doi.org/10.1128/mr.46.1.43-70.1982.

Kool, D.M., Wrage, N., Zechmeister-Boltenstern, S., Pfeffer, M., Brus, D., Oenema, O., Van Groenigen, J.W., 2010. Nitrifier denitrification can be a source of N_2O from soil: a revised approach to the dual-isotope labelling method. European Journal of Soil Science 61, 759–772. https://doi.org/10.1111/j.1365-2389.2010.01270.x.

Kuypers, M.M.M., Marchant, H.K., Kartal, B., 2018. The microbial nitrogen-cycling network. Nature Reviews Microbiology 16, 263–276. https://doi.org/10.1038/nrmicro.2018.9.

Kuzyakov, Y., 2006. Sources of CO2 efflux from soil and review of partitioning methods. Soil Biology and Biochemistry 38, 425–448. https://doi.org/10.1016/j.soilbio.2005.08.020.

Kuzyakov, Y., Xu, X., 2013. Competition between roots and microorganisms for nitrogen: mechanisms and ecological relevance. New Phytologist 198, 656–669. https://doi.org/10.1111/nph.12235.

Laine, M., Rütting, T., Alakukku, L., Palojärvi, A., Strömmer, R., 2018. Process rates of nitrogen cycle in uppermost topsoil after harvesting in no-tilled and ploughed agricultural clay soil. Nutrient Cycling in Agroecosystems 110, 39–49. https://doi.org/10.1007/s10705-017-9825-2.

Lama, S., Kuhn, T., Lehmann, M.F., Müller, C., Gonzalez, O., Eisenhauer, N., Lange, M., Scheu, S., Oelmann, Y., Wilcke, W., 2020. The biodiversity - N cycle relationship: a

^{15}N tracer experiment with soil from plant mixtures of varying diversity to model N pool sizes and transformation rates. Biology and Fertility of Soils 56, 1047–1061. https://doi.org/10.1007/s00374-020-01480-x.

Laughlin, R.J., Stevens, R.J., 2002. Evidence for fungal dominance of denitrification and codenitrification in a grassland soil. Soil Science Society of America Journal 66, 1540–1548. https://doi.org/10.2136/sssaj2002.1540.

Lenth, R.V., 2023. Emmeans: Estimated Marginal Means, Aka Least-Squares Means, 1.8.7 ed.

Lewicka-Szczebak, D., Well, R., Giesemann, A., Rohe, L., Wolf, U., 2013. An enhanced technique for automated determination of ^{15}N signatures of N_2, (N_2+N_2O) and N_2O in gas samples. Rapid Communications in Mass Spectrometry 27, 1548–1558. https://doi.org/10.1002/rcm.6605.

Lewicka-Szczebak, D., Well, R., Köster, J.R., Fuß, R., Senbayram, M., Dittert, K., Flessa, H., 2014. Experimental determinations of isotopic fractionation factors associated with N_2O production and reduction during denitrification in soils. Geochimica et Cosmochimica Acta 134, 55–73. https://doi.org/10.1016/j.gca.2014.03.010.

Li, C., Hu, H.-W., Chen, Q.-L., Chen, D., He, J.-Z., 2019. Comammox Nitrospira play an active role in nitrification of agricultural soils amended with nitrogen fertilizers. Soil Biology and Biochemistry 138. https://doi.org/10.1016/j.soilbio.2019.107609.

Li, C., Yan, K., Tang, L., Jia, Z., Li, Y., 2014. Change in deep soil microbial communities due to long-term fertilization. Soil Biology and Biochemistry 75, 264–272. https://doi.org/10.1016/j.soilbio.2014.04.023.

Linn, D.M., Doran, J.W., 1984. Effect of water-filled pore space on carbon dioxide and nitrous oxide production in tilled and nontilled soils. Soil Science Society of America Journal 48, 1267–1272. https://doi.org/10.2136/sssaj1984.03615995004800060013x.

Long, A., Heitman, J., Tobias, C., Philips, R., Song, B., 2013. Co-occurring anammox, denitrification, and codenitrification in agricultural soils. Applied and Environmental Microbiology 79, 168–176. https://doi.org/10.1128/aem.02520-12.

Lu, M., Zhou, X., Luo, Y., Yang, Y., Fang, C., Chen, J., Li, B., 2011. Minor stimulation of soil carbon storage by nitrogen addition: a meta-analysis. Agriculture, Ecosystems & Environment 140, 234–244. https://doi.org/10.1016/j.agee.2010.12.010.

Ma, W., Tang, S., Dengzeng, Z., Zhang, D., Zhang, T., Ma, X., 2022. Root exudates contribute to belowground ecosystem hotspots: a review. Frontiers in Microbiology 13. https://doi.org/10.3389/fmicb.2022.937940.

Malhi, S.S., Johnston, A.M., Gill, K.S., Pennock, D.J., 2004. Landscape position effects on the recovery of15N-labelled urea applied to wheat on two soils in Saskatchewan, Canada. Nutrient Cycling in Agroecosystems 68, 85–93. https://doi.org/10.1023/B:FRES.0000012238.02635.7e.

McCarty, G.W., Bremner, J.M., 1992. Availability of organic carbon for denitrification of nitrate in subsoils. Biology and Fertility of Soils 14, 219–222. https://doi.org/10.1007/bf00346064.

Medinets, S., Skiba, U., Rennenberg, H., Butterbach-Bahl, K., 2015. A review of soil NO transformation: associated processes and possible physiological significance on organisms. Soil Biology and Biochemistry 80, 92–117. https://doi.org/10.1016/j.soilbio.2014.09.025.

Mooshammer, M., Wanek, W., Hämmerle, I., Fuchslueger, L., Hofhansl, F., Knoltsch, A., Schnecker, J., Takriti, M., Watzka, M., Wild, B., Keiblinger, K.M., Zechmeister-Boltenstern, S., Richter, A., 2014. Adjustment of microbial nitrogen use efficiency to carbon:nitrogen imbalances regulates soil nitrogen cycling. Nature Communications 5. https://doi.org/10.1038/ncomms4694.

Müller, C., Laughlin, R.J., Christie, P., Watson, C.J., 2011. Effects of repeated fertilizer and cattle slurry applications over 38 years on N dynamics in a temperate grassland soil. Soil Biology and Biochemistry 43, 1362–1371. https://doi.org/10.1016/j.soilbio.2011.03.014.

Müller, C., Rütting, T., Kattge, J., Laughlin, R.J., Stevens, R.J., 2007. Estimation of parameters in complex 15N tracing models by Monte Carlo sampling. Soil Biology and Biochemistry 39, 715–726. https://doi.org/10.1016/j.soilbio.2006.09.021.

Müller, C., Stevens, R.J., Laughlin, R.J., 2004. A ^{15}N tracing model to analyse N transformations in old grassland soil. Soil Biology and Biochemistry 36, 619–632. https://doi.org/10.1016/j.soilbio.2003.12.006.

Mulvaney, R.L., Khan, S.A., Mulvaney, C.S., 1997. Nitrogen fertilizers promote denitrification. Biology and Fertility of Soils 24, 211–220. https://doi.org/10.1007/s003740050233.

Murphy, D.V., Recous, S., Stockdale, E.A., Fillery, I.R.P., Jensen, L.S., Hatch, D.J., Goulding, K.W.T., 2003. Gross nitrogen fluxes in soil : theory, measurement and application of ^{15}N pool dilution techniques. Advances in Agronomy 79, 69–118.

Myrold, D.D., 2021. Transformations of nitrogen, principles and applications of. Soil Microbiology 385–421.

Norton, J., Ouyang, Y., 2019. Controls and adaptive management of nitrification in agricultural soils. Frontiers in Microbiology 10, 1931. https://doi.org/10.3389/fmicb.2019.01931.

O'Neill, M., Gallego-Lorenzo, L., Lanigan, G.J., Forristal, P.D., Osborne, B.A., 2020. Assessment of nitrous oxide emission factors for arable and grassland ecosystems. Journal of Integrative Environmental Sciences 17, 165–185. https://doi.org/10.1080/1943815x.2020.1825227.

Payton, M.E., Miller, A.E., Raun, W.R., 2000. Testing statistical hypotheses using standard error bars and confidence intervals. Communications in Soil Science and Plant Analysis 31, 547–551. https://doi.org/10.1080/00103620009370458.

Pfülb, L., Elsgaard, L., Dörsch, P., Fuß, R., Well, R., 2024. Impact of liming and maize residues on N2O and N2 fluxes in agricultural soils: an incubation study. Biology and Fertility of Soils. https://doi.org/10.1007/s00374-024-01825-w.

Pradhan, R., Izaurralde, R.C., Nyborg, M., Malhi, S.S., 1997. Yield and N uptake of barley on two artificially eroded soils in north-central Alberta. Canadian Journal of Soil Science 77, 317–322. https://doi.org/10.4141/s96-006.

Preusser, S., Poll, C., Marhan, S., Angst, G., Mueller, C.W., Bachmann, J., Kandeler, E., 2019. Fungi and bacteria respond differently to changing environmental conditions within a soil profile. Soil Biology and Biochemistry 137. https://doi.org/10.1016/j.soilbio.2019.107543.

Putz, M., Schleusner, P., Rütting, T., Hallin, S., 2018. Relative abundance of denitrifying and DNRA bacteria and their activity determine nitrogen retention or loss in agricultural soil. Soil Biology and Biochemistry 123, 97–104. https://doi.org/10.1016/j.soilbio.2018.05.006.

Quinton, J.N., Govers, G., Van Oost, K., Bardgett, R.D., 2010. The impact of agricultural soil erosion on biogeochemical cycling. Nature Geoscience 3, 311–314. https://doi.org/10.1038/ngeo838.

R Core Team, 2023. R: A Language and Environment for Statistical Computing. R Foundation for Statistical Computing, Vienna, Austria.

Reicosky, D., Lindstrom, M., Schumacher, T., Lobb, D., Malo, D., 2005. Tillage-induced CO loss across an eroded landscape. Soil and Tillage Research 81, 183–194. https://doi.org/10.1016/j.still.2004.09.007.

Reicosky, D.C., 1997. Tillage-induced CO_2 emission from soil. Nutrient Cycling in Agroecosystems 49, 273–285. https://doi.org/10.1023/a:1009766510274.

Roberts, W.P., Chan, K.Y., 1990. Tillage-induced increases in carbon dioxide loss from soil. Soil and Tillage Research 17, 143–151. https://doi.org/10.1016/0167-1987(90)90012-3.

Robertson, G.P., Groffman, P.M., 2015. Nitrogen Transformations, Soil Microbiology, Ecology and Biochemistry, pp. 421–446.

Robertson, G.P., Groffman, P.M., 2024. Nitrogen Transformations, Soil Microbiology, Ecology and Biochemistry, pp. 407–438.

Robertson, G.P., Tiedje, J.M., 1987. Nitrous oxide sources in aerobic soils: nitrification, denitrification and other biological processes. Soil Biology and Biochemistry 19, 187–193. https://doi.org/10.1016/0038-0717(87)90080-0.

Rohe, L., Apelt, B., Vogel, H.-J., Well, R., Wu, G.-M., Schlüter, S., 2021. Denitrification in soil as a function of oxygen availability at the microscale. Biogeosciences 18, 1185–1201. https://doi.org/10.5194/bg-18-1185-2021.

Rummel, P.S., Well, R., Pfeiffer, B., Dittert, K., Floßmann, S., Pausch, J., 2021. Nitrate uptake and carbon exudation – do plant roots stimulate or inhibit denitrification? Plant and Soil 459, 217–233. https://doi.org/10.1007/s11104-020-04750-7.

Ruser, R., Flessa, H., Russow, R., Schmidt, G., Buegger, F., Munch, J.C., 2006. Emission of N_2O, N_2 and CO_2 from soil fertilized with nitrate: effect of compaction, soil moisture and rewetting. Soil Biology and Biochemistry 38, 263–274. https://doi.org/10.1016/j.soilbio.2005.05.005.

Russow, R., Spott, O., Stange, C.F., 2008. Evaluation of nitrate and ammonium as sources of NO and N_2O emissions from black earth soils (Haplic Chernozem) based on ^{15}N field experiments. Soil Biology and Biochemistry 40, 380–391. https://doi.org/10.1016/j.soilbio.2007.08.020.

Rütting, T., Boeckx, P., Müller, C., Klemedtsson, L., 2011a. Assessment of the importance of dissimilatory nitrate reduction to ammonium for the terrestrial nitrogen cycle. Biogeosciences 8, 1779–1791. https://doi.org/10.5194/bg-8-1779-2011.

Rütting, T., Huygens, D., Staelens, J., Muller, C., Boeckx, P., 2011b. Advances in 15N-tracing experiments: new labelling and data analysis approaches. Biochemical Society Transactions 39, 279–283. https://doi.org/10.1042/BST0390279.

Rütting, T., Müller, C., 2007. ^{15}N tracing models with a Monte Carlo optimization procedure provide new insights on gross N transformations in soils. Soil Biology and Biochemistry 39, 2351–2361. https://doi.org/10.1016/j.soilbio.2007.04.006.

Sainju, U.M., Stevens, W.B., Caesar-TonThat, T., Liebig, M.A., 2012. Soil greenhouse gas emissions affected by irrigation, tillage, crop rotation, and nitrogen fertilization. Journal of Environmental Quality 41, 1774–1786. https://doi.org/10.2134/jeq2012.0176.

Schlüter, S., Henjes, S., Zawallich, J., Bergaust, L., Horn, M., Ippisch, O., Vogel, H.-J., Dörsch, P., 2018. Denitrification in soil aggregate analogues-effect of aggregate size and oxygen diffusion. Frontiers in Environmental Science 6. https://doi.org/10.3389/fenvs.2018.00017.

Schlüter, S., Lucas, M., Grosz, B., Ippisch, O., Zawallich, J., He, H., Dechow, R., Kraus, D., Blagodatsky, S., Senbayram, M., Kravchenko, A., Vogel, H.-J., Well, R., 2024. The anaerobic soil volume as a controlling factor of denitrification: a review. Biology and Fertility of Soils. https://doi.org/10.1007/s00374-024-01819-8.

Schmidt, C.S., Richardson, D.J., Baggs, E.M., 2011. Constraining the conditions conducive to dissimilatory nitrate reduction to ammonium in temperate arable soils. Soil Biology and Biochemistry 43, 1607–1611. https://doi.org/10.1016/j.soilbio.2011.02.015.

Schrumpf, M., Kaiser, K., Guggenberger, G., Persson, T., Kögel-Knabner, I., Schulze, E.D., 2013. Storage and stability of organic carbon in soils as related to depth, occlusion within aggregates, and attachment to minerals. Biogeosciences 10, 1675–1691. https://doi.org/10.5194/bg-10-1675-2013.

Senbayram, M., Budai, A., Bol, R., Chadwick, D., Marton, L., Gündogan, R., Wu, D., 2019. Soil NO_3^- level and O_2 availability are key factors in controlling N_2O reduction to N_2 following long-term liming of an acidic sandy soil. Soil Biology and Biochemistry 132, 165–173. https://doi.org/10.1016/j.soilbio.2019.02.009.

Senbayram, M., Chen, R., Mühling, K.H., Dittert, K., 2009. Contribution of nitrification and denitrification to nitrous oxide emissions from soils after application of biogas waste and other fertilizers. Rapid Communications in Mass Spectrometry 23, 2489–2498. https://doi.org/10.1002/rcm.4067.

Senbayram, M., Well, R., Shan, J., Bol, R., Burkart, S., Jones, D.L., Wu, D., 2020. Rhizosphere processes in nitrate-rich barley soil tripled both N_2O and N_2 losses due to enhanced bacterial and fungal denitrification. Plant and Soil 448, 509–522. https://doi.org/10.1007/s11104-020-04457-9.

Smith, P., Martino, D., Cai, Z., Gwary, D., Janzen, H., Kumar, P., McCarl, B., Ogle, S., O'Mara, F., Rice, C., Scholes, B., Sirotenko, O., Howden, M., McAllister, T., Pan, G., Romanenkov, V., Schneider, U., Towprayoon, S., Wattenbach, M., Smith, J., 2007.

Greenhouse gas mitigation in agriculture. Philosophical Transactions of the Royal Society B: Biological Sciences 363, 789–813. https://doi.org/10.1098/rstb.2007.2184.

Soong, J.L., Fuchslueger, L., Marañon-Jimenez, S., Torn, M.S., Janssens, I.A., Penuelas, J., Richter, A., 2020. Microbial carbon limitation: the need for integrating microorganisms into our understanding of ecosystem carbon cycling. Global Change Biology 26, 1953–1961. https://doi.org/10.1111/gcb.14962.

Spott, O., Russow, R., Apelt, B., Stange, C.F., 2006. A ^{15}N-aided artificial atmosphere gas flow technique for online determination of soil N_2 release using the zeolite Kostrolith SX6. Rapid Communications in Mass Spectrometry 20, 3267–3274. https://doi.org/10.1002/rcm.2722.

Spott, O., Russow, R., Stange, C.F., 2011. Formation of hybrid N_2O and hybrid N_2 due to codenitrification: first review of a barely considered process of microbially mediated N-nitrosation. Soil Biology and Biochemistry 43, 1995–2011. https://doi.org/10.1016/j.soilbio.2011.06.014.

Spott, O., Stange, C.F., 2007. A new mathematical approach for calculating the contribution of anammox, denitrification and atmosphere to an N_2 mixture based on a ^{15}N tracer technique. Rapid Communications in Mass Spectrometry 21, 2398–2406. https://doi.org/10.1002/rcm.3098.

Spott, O., Stange, C.F., 2011. Formation of hybrid N_2O in a suspended soil due to co-denitrification of NH_2OH. Journal of Plant Nutrition and Soil Science 174, 554–567. https://doi.org/10.1002/jpln.201000200.

The MathWorks Inc, 2021. MATLAB Version XX (R2021a), vol. XX. The MathWorks Inc, Natick, Massachusetts, p. R2021a.

Tiedje, J.M., Sexstone, A.J., Myrold, D.D., Robinson, J.A., 1982. Denitrification: ecological niches, competition and survival. Antonie van Leeuwenhoek 48, 569–583. https://doi.org/10.1007/bf00399542.

Tiedje, J.M., 1988. Ecology of denitrification and dissimilatory nitrate reduction. Biology of anaerobic organisms 179–244.

Vaidya, S., Hoffmann, M., Dubbert, M., Kramp, K., Schmidt, M., Verch, G., Sommer, M., Augustin, J., 2024. Topsoil dilution by subsoil admixture had less impact on soil organic carbon stock development than fertilizer form and erosion state. Science of The Total Environment 946. https://doi.org/10.1016/j.scitotenv.2024.174243.

Vaidya, S., Hoffmann, M., Holz, M., Macagga, R., Monzon, O., Thalmann, M., Jurisch, N., Pehle, N., Verch, G., Sommer, M., Augustin, J., 2023. Similar strong impact of N fertilizer form and soil erosion state on N_2O emissions from croplands. Geoderma 429. https://doi.org/10.1016/j.geoderma.2022.116243.

Van Oost, K., Govers, G., Quine, T.A., Heckrath, G., Olesen, J.E., De Gryze, S., Merckx, R., 2005. Landscape-scale modeling of carbon cycling under the impact of soil redistribution: the role of tillage erosion. Global Biogeochemical Cycles 19. https://doi.org/10.1029/2005gb002471.

Van Oost, K., Quine, T.A., Govers, G., De Gryze, S., Six, J., Harden, J.W., Ritchie, J.C., McCarty, G.W., Heckrath, G., Kosmas, C., Giraldez, J.V., da Silva, J.R.M., Merckx, R., 2007. The impact of agricultural soil erosion on the global carbon cycle. Science 318, 626–629. https://doi.org/10.1126/science.1145724.

Wang, Z., Wang, R., Sun, Q., Du, L., Zhao, M., Hu, Y., Guo, S., 2017. Soil CO_2 emissions from different slope gradients and positions in the semiarid Loess Plateau of China. Ecological Engineering 105, 231–239. https://doi.org/10.1016/j.ecoleng.2017.04.050.

Watkins, N., Barraclough, D., 1996. Gross rates of N mineralization associated with the decomposition of plant residues. Soil Biology and Biochemistry 28, 169–175. https://doi.org/10.1016/0038-0717(95)00123-9.

Watt, M.P., Cresswell, C.F., 1987. A comparison between the utilization of storage protein and exogenous nitrate during seedling establishment in Zea mays L. Plant, Cell and Environment 10, 327–332. https://doi.org/10.1111/j.1365-3040.1987.tb01613.x.

Weintraub, S.R., Taylor, P.G., Porder, S., Cleveland, C.C., Asner, G.P., Townsend, A.R., 2015. Topographic controls on soil nitrogen availability in a lowland tropical forest. Ecology 96, 1561–1574. https://doi.org/10.1890/14-0834.1.

Well, R., Burkart, S., Giesemann, A., Grosz, B., Koster, J.R., Lewicka-Szczebak, D., 2019. Improvement of the ^{15}N gas flux method for in situ measurement of soil denitrification and its product stoichiometry. Rapid Communications in Mass Spectrometry 33, 437–448. https://doi.org/10.1002/rcm.8363.

Wickham, H., 2016. ggplot2: Elegant Graphics for Data Analysis. Springer-Verlag, New York.

Wrage-Mönnig, N., Horn, M.A., Well, R., Müller, C., Velthof, G., Oenema, O., 2018. The role of nitrifier denitrification in the production of nitrous oxide revisited. Soil Biology and Biochemistry 123, A3–A16. https://doi.org/10.1016/j.soilbio.2018.03.020.

Wrage, N., Velthof, G.L., van Beusichem, M.L., Oenema, O., 2001. Role of nitrifier denitrification in the production of nitrous oxide. Soil Biology and Biochemistry 33, 1723–1732. https://doi.org/10.1016/s0038-0717(01)00096-7.

Yang, L., Zhang, X., Ju, X., Wu, D., 2021. Oxygen-depletion by rapid ammonia oxidation regulates kinetics of N_2O, NO and N_2 production in an ammonium fertilised agricultural soil. Soil Biology and Biochemistry 163. https://doi.org/10.1016/j.soilbio.2021.108460.

Yankelzon, I., Willibald, G., Dannenmann, M., Malique, F., Ostler, U., Scheer, C., Butterbach-Bahl, K., 2024. A new incubation system to simultaneously measure N2 as well as N2O and CO2 fluxes from plant-soil mesocosms. Biology and Fertility of Soils. https://doi.org/10.1007/s00374-024-01809-w.

Zentgraf, I., Hoffmann, M., Augustin, J., Buchen-Tschiskale, C., Hoferer, S., Holz, M., 2024. Effect of mineral and organic fertilizer on N dynamics upon erosion-induced topsoil dilution. Heliyon 10, e34822. https://doi.org/10.1016/j.heliyon.2024.e34822.

Zhu, X., Burger, M., Doane, T.A., Horwath, W.R., 2013. Ammonia oxidation pathways and nitrifier denitrification are significant sources of N_2O and NO under low oxygen availability. Proceedings of the National Academy of Sciences 110, 6328–6333. https://doi.org/10.1073/pnas.1219993110.